High-resolution study of $T_z = +2 \rightarrow +1$ Gamow-Teller transitions in the ^{44}Ca(^{3}He,t)^{44}Sc reaction

Y. Fujita,[1,2,*] T. Adachi,[2] H. Fujita,[1,2] A. Algora,[3,4] B. Blank,[5] M. Csatlós,[4] J. M. Deaven,[6,7,8] E. Estevez-Aguado,[3] E. Ganioğlu,[9] C. J. Guess,[6,7,8,†] J. Gulyás,[4] K. Hatanaka,[2] K. Hirota,[2] M. Honma,[10] D. Ishikawa,[2] A. Krasznahorkay,[4] H. Matsubara,[2,‡] R. Meharchand,[6,7,8,§] F. Molina,[3,‖] H. Okamura,[2,¶] H. J. Ong,[2] T. Otsuka,[11] G. Perdikakis,[6,7,8] B. Rubio,[3] C. Scholl,[12,**] Y. Shimbara,[13,††] E. J. Stephenson,[14] G. Susoy,[9] T. Suzuki,[2] A. Tamii,[2] J. H. Thies,[15] R. G. T. Zegers,[6,7,8] and J. Zenihiro[2,‡‡]

[1]*Department of Physics, Osaka University, Toyonaka, Osaka 560-0043, Japan*
[2]*Research Center for Nuclear Physics, Osaka University, Ibaraki, Osaka 567-0047, Japan*
[3]*Instituto de Física Corpuscular, CSIC–Universidad de Valencia, E-46071 Valencia, Spain*
[4]*Institute of Nuclear Research (ATOMKI), Post Office Box 51, H-4001 Debrecen, Hungary*
[5]*Centre d'Etudes Nucléaires de Bordeaux Gradignan, Université Bordeaux 1, UMR 5797 CNRS/IN2P3, B.P. 120, F-33175 Gradignan, France*
[6]*National Superconducting Cyclotron Laboratory, Michigan State University, East Lansing, Michigan 48824-1321, USA*
[7]*Joint Institute for Nuclear Astrophysics, Michigan State University, East Lansing, Michigan 48824, USA*
[8]*Department of Physics and Astronomy, Michigan State University, East Lansing, Michigan 48824, USA*
[9]*Department of Physics, Istanbul University, Istanbul 34134, Turkey*
[10]*Center for Mathematical Science, University of Aizu, Aizu-Wakamatsu, Fukushima 965-8580, Japan*
[11]*Department of Physics, University of Tokyo, Hongo, Bunkyo, Tokyo 113-0033, Japan*
[12]*Institut für Kernphysik, Universität zu Köln, 50937 Köln, Germany*
[13]*Graduate School of Science and Technology, Niigata University, Nishi, Niigata 950-2181, Japan*
[14]*Center for Exploration of Energy and Matter, Indiana University, Bloomington, Indiana 47408 USA*
[15]*Institut für Kernphysik, Westfälische Wilhelms-Universität, D-48149 Münster, Germany*

(Received 14 April 2013; revised manuscript received 13 June 2013; published 11 July 2013)

In order to study the Gamow-Teller (GT) transitions from the $T_z = +2$ nucleus ^{44}Ca to the $T_z = +1$ nucleus ^{44}Sc, where T_z is the z component of isospin T, we performed the (p, n)-type (^{3}He, t) charge-exchange (CE) reaction at 140 MeV/nucleon and the scattering angles 0° and 2.5°. An energy resolution of 28 keV, that was realized by applying matching techniques to the magnetic spectrometer system, allowed the study of fragmented states. The GT transition strengths, B(GT), were derived up to the excitation energy (E_x) of 13.7 MeV assuming the proportionality between cross sections and B(GT) values. The total sum of B(GT) values in discrete states was 3.7, which was 31% of the sum-rule-limit value of 12. Shell model calculations using the GXPF1J interaction could reproduce the gross features of the experimental B(GT) distribution, but not the fragmentation of the strength. By introducing the concepts of isospin, properties of isospin analogous transitions and states were investigated. (i) Assuming isospin symmetry, the $T_z = +2 \rightarrow +1$ and $T_z = -2 \rightarrow -1$ mirror GT transitions should have the same properties, where the latter can be studied in the β decay of ^{44}Cr to ^{44}V. First, we confirmed that the β-decay half-life $T_{1/2}$ of ^{44}Cr can be reproduced using the B(GT) distribution from the ^{44}Ca(^{3}He, t) measurement. Then, the 0°, (^{3}He, t) spectrum was modified to deduce the "β-decay spectrum" and it was compared with the delayed-proton spectrum from the ^{44}Cr β decay. The two spectra were mostly in agreement for the GT excitations, but suppression of the proton decay was found for the $T = 2$ isobaric analog state (IAS). (ii) Starting from the $T = 2$ ground state of ^{44}Ca, the (^{3}He, t) can excite GT states (state populated by GT transitions) with $T = 1$, 2, and 3. On the other hand, the ^{44}Ca(p, p') reaction can excite spin-$M1$ states (states populated by spin-$M1$ transitions) with $T = 2$ and 3 that are analogous to the $T = 2$ and 3 GT states, respectively. By comparing the spectra from these two reactions, a T value of 2 is suggested for several GT states in the $E_x = 11.5$–13.7 MeV region. (iii) It has been suggested that the $T = 2$, $J^\pi = 0^+$ double isobaric analog state (DIAS) at 9.338 MeV in the $T_z = 0$ nucleus ^{44}Ti forms an isospin-mixed doublet with a subsidiary 0^+ state at 9.298 MeV. Since no corresponding state was found in the $T_z = +1$ nucleus ^{44}Sc, we suggest $T = 0$ for the subsidiary state.

DOI: 10.1103/PhysRevC.88.014308 PACS number(s): 21.10.Hw, 25.55.Kr, 23.40.−s, 27.40.+z

*fujita@rcnp.osaka-u.ac.jp
†Present address: Department of Physics and Applied Physics, University of Massachusetts Lowell, Lowell, Massachusetts 01854, USA.
‡Present address: NIRS, Inage, Chiba 263-8555, Japan.
§Present address: Los Alamos National Laboratory, Los Alamos, New Mexico 87545, USA.
‖Present address: Comisión Chilena de Energía Nuclear, Post Office Box 188-D, Santiago, Chile.
¶Deceased.
**Present address: Institute for Work Design of North Rhine-Westphalia, Radiation Protection Services, 40225 Düsseldorf, Germany.
††Present address: CYRIC, Tohoku University, Aramaki, Aoba, Sendai 980-8578, Japan.

I. INTRODUCTION

Gamow-Teller (GT) transitions are mediated by the $\sigma\tau$ operator. Therefore, GT transitions are characterized by an angular momentum transfer $\Delta L = 0$ and spin-isospin flip ($\Delta S = 1$ and $\Delta T = 1$). Due to this simple character, GT transitions are important tools for the study of nuclear structures [1–4]. In addition, GT transitions are the most common nuclear weak-interaction processes in stellar evolution and nucleosynthesis [5]. In the core-collapse stage of type II supernovae, weak interaction processes of pf-shell nuclei play important roles. In addition, rp-process nucleosynthesis responsible for the generation of many heavy proton-rich elements proceeds through proton-rich pf-shell nuclei. Therefore, the study of GT transitions starting not just from stable but also unstable pf-shell nuclei is of key importance in nuclear astrophysics. However, our knowledge of these GT transitions is relatively poor [5].

A. Study of Gamow-Teller transitions by charge-exchange reactions and β decay

Experimental studies of β decay can provide the most direct information on the GT transition strength B(GT). However, the excitation energies in final nuclei accessible in β decays are limited by the decay Q values. In addition, the study of the transitions to higher excited states is difficult, because the phase-space factor decreases with the excitation energy (E_x) [3,4]. Therefore, most of the β^+-decay studies for proton-rich pf-shell nuclei having $T_z = -1$, $-3/2$, or -2, where T_z is the z component of isospin T defined by $(1/2)(N - Z)$, still struggle to derive B(GT) values for transitions to higher excited states [4]. However, assuming isospin symmetry for mirror transitions, the GT transitions from proton-rich pf-shell nuclei can be deduced by studying the mirror GT transitions from $T_z = +1$, $+3/2$, or $+2$ stable nuclei using (p, n)-type charge-exchange (CE) reactions. In addition, one can observe GT transitions to states at higher excitation energies without the Q-value limitation [2,6].

In CE reactions, GT excitations become prominent at intermediate incident energies (above 100 MeV/nucleon) and forward angles around 0°. In addition, under these conditions there is a close proportionality between the GT cross sections and the B(GT) values [7,8],

$$\sigma^{\mathrm{GT}}(q,\omega) \simeq K(\omega) N_{\sigma\tau} |J_{\sigma\tau}(q)|^2 B(\mathrm{GT}) \quad (1)$$

$$= \hat{\sigma}^{\mathrm{GT}} F(q,\omega) B(\mathrm{GT}), \quad (2)$$

where $J_{\sigma\tau}(q)$ is the volume integral of the effective interaction $V_{\sigma\tau}$ at momentum transfer q (≈ 0), $K(\omega)$ is the kinematic factor, ω is the total energy transfer, and $N_{\sigma\tau}$ is a distortion factor. The value $\hat{\sigma}^{\mathrm{GT}}$ is the unit cross section for the GT transition at $q = \omega = 0$ and a given incoming energy for a system with mass number A. The value $F(q,\omega)$ gives the dependence of the GT cross sections on the momentum and energy transfers. It has a value of unity at $q = \omega = 0$ and usually decreases gradually as a function of E_x, and can be reliably obtained from distorted-wave Born approximation (DWBA) calculations.

Since the 1980s, (p, n) reactions performed at proton incoming energies $E_p = 120$–200 MeV were used for the study of GT transitions in the β^- direction [6]. One important finding was the bump-like structures with concentrated GT strength at high excitation energies of $E_x = 9$–18 MeV, structures named the Gamow-Teller resonance (GTR). GTRs have been systematically observed in pf-shell and heavier nuclei. The energy resolutions achieved in the (p, n) reactions were around 300 keV or greater.

The advantage of using the $(^3\mathrm{He}, t)$ reaction is that a higher energy resolution can be achieved. At the Research Center for Nuclear Physics (RCNP), Osaka, resolutions of ≈ 30 keV have been achieved at the ^{3}He beam energy of 140 MeV/nucleon. Recent studies of GTRs on $T_z = +1$ nuclei ^{54}Fe [9] and ^{58}Ni [10] have shown that the bump-like structures observed in (p, n) studies actually consist of many discrete states excited by GT transitions (GT states). The fragmentation of GT strength was also observed in a recent study on the $T_z = +3/2$ nucleus ^{47}Ti [11]. In addition, the close proportionality expressed in Eq. (2) has been demonstrated to hold for $\Delta L = 0$ transitions with $B(\mathrm{GT}) \geqslant 0.04$, with deviations of a few percent to 10% in studies of the $A = 23$, 26, and 27 nuclear systems [12–16]. (Note that poorer agreement was also found in some specific cases; see the discussions in Ref. [4]). In these mass A systems, the strengths of multiple, analogous GT transitions with $T_z = \pm 1/2 \rightarrow \mp 1/2$ or $T_z = \pm 1 \rightarrow 0$ could be compared in the $(^3\mathrm{He}, t)$ and β-decay studies.

In this paper, we report the study of GT transitions leading to states up to $E_x = 13.7$ MeV in the $T_z = +1$ nucleus ^{44}Sc from the $T_z = +2$ nucleus ^{44}Ca using the $(^3\mathrm{He}, t)$ reaction. The GT transitions from $T_z = +2$, pf-shell nuclei ^{52}Cr, ^{56}Fe, and ^{60}Ni were previously studied in (p, n) reactions at 120 and 160 MeV [17,18] and GTRs were observed in all of the final nuclei ^{52}Mn, ^{56}Co, and ^{60}Cu. On the other hand, the ^{44}Ca$(p, n)^{44}$Sc spectrum [6] does not show the bump-like structure associated with the GTR; the GT strength was mainly concentrated in the lower energy region of $E_x < 7$ MeV, where discrete states are expected. Accordingly, the detailed study of the GT transitions starting from the lightest $T_z = +2$, pf-shell nucleus ^{44}Ca is of interest.

B. Isospin symmetry of mirror transitions

The idea of nuclear isospin symmetry comes from the fact that protons and neutrons behave in almost the same way in terms of the strong interaction that plays a "major" role in determining the nuclear structure, although the "minor" electromagnetic interaction represented by the Coulomb force violates the symmetry. Under the assumption of isospin symmetry, an analogous structure is expected for isobaric nuclei with the same A but with different T_z (see e.g., Refs. [4,19,20]). The corresponding states in isobars are called isobaric analog states (or simply analog states), and are expected to have the same nuclear structure. Transitions between corresponding analog states are also analogous and have corresponding strengths.

[‡‡] Present address: RIKEN Nishina Center, Wako, Saitama 351-0198, Japan.

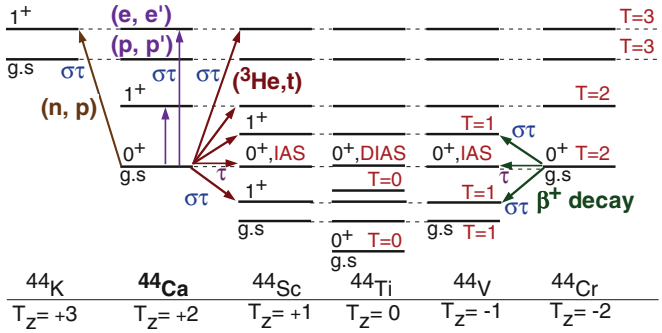

FIG. 1. (Color online) Schematic view of the analog states (connected by dashed lines) and analogous transitions in the mass $A = 44$, $T_z = +3$, $+2$, $+1$, 0, -1, and -2 isobaric system. The Coulomb displacement energies are removed so that the isospin symmetry of analog states and analogous transitions becomes clearer. In this scheme, the inclined arrows show the $0^+ \rightarrow 1^+$, GT transitions caused by the $\sigma\tau$-type operator from the ground states of mirror nuclei ^{44}Ca and ^{44}Cr. On the other hand, the analogous $0^+ \rightarrow 0^+$ Fermi transitions to the IASs governed by the τ-type operator are shown by the horizontal arrows. The vertical arrows show the $0^+ \rightarrow 1^+$ transitions caused by inelastic-type reactions such as (p, p') or (e, e') on ^{44}Ca. The isobaric analog state in ^{44}Ti is called the double isobaric analog state (DIAS).

In the $A = 44$, $T = 2$ quintet system, GT and Fermi transitions from the $J^\pi = 0^+$ ground states of the $T_z = \pm 2$ even-even nuclei ^{44}Ca and ^{44}Cr to 1^+ states (GT states) and the 0^+, $T = 2$ isobaric analog state (IAS) in the $T_z = \pm 1$, odd-odd nuclei ^{44}Sc and ^{44}V are analogous (see Fig. 1). In the *sd*- and *pf*-shell region, $T_z = -2 \rightarrow -1$, GT and Fermi transitions can be studied in β decay, but our current knowledge of these decays is rather poor. On the other hand, $T_z = +2 \rightarrow +1$ transitions can be studied using the $(^3\mathrm{He}, t)$ reaction precisely. Therefore, assuming isospin symmetry, we can deduce details of the very exotic $T_z = -2 \rightarrow -1$ transitions from studies of the $T_z = +2 \rightarrow +1$ transitions starting from stable nuclei. We will examine the similarity of these mirror transitions by comparing the β-delayed proton spectrum studied in the ^{44}Cr β decay [21] and the ^{44}Ca$(^3\mathrm{He}, t)$ spectrum. We also examine how well the β-decay half-life $T_{1/2}$ of ^{44}Cr can be reproduced from the distribution of the Fermi and GT transition strengths studied in the ^{44}Ca$(^3\mathrm{He}, t)$, CE reaction.

We see from Fig. 1, that proton inelastic scattering ^{44}Ca(p, p') and electron inelastic scattering ^{44}Ca(e, e') can excite 1^+ states in ^{44}Ca that are analogous to GT states in ^{44}Sc. We discuss the values of isospin T for the excited GT states by comparing the spectra from our ^{44}Ca$(^3\mathrm{He}, t)$, CE reaction and the ^{44}Ca(p, p') measurement.

II. EXPERIMENT

The ^{44}Ca$(^3\mathrm{He}, t)^{44}$Sc experiment was carried out at the high-resolution facility of RCNP [22], consisting of the "WS course" beam line [23] and the "Grand Raiden" spectrometer [24] using a 140 MeV/nucleon ^{3}He beam from the $K = 400$ Ring Cyclotron [22]. The measurements were performed at two spectrometer angles of 0° and 2.5°. In the 0° measurement, both the $^3\mathrm{He}^{2+}$ beam and the tritons entered in the first dipole magnet (D1 magnet) of the spectrometer. Since the $^3\mathrm{He}^{2+}$ beam, with a magnetic rigidity $B\rho$ of about half of the tritons, has a much smaller bending radius, it was stopped in a Faraday cup placed inside the D1 magnet. In the measurement at 2.5°, the $^3\mathrm{He}^{2+}$ beam was stopped in a Faraday cup placed just after the first quadrupole magnet (Q1 magnet) of the spectrometer.

The target was a self-supporting foil of enriched (98.8%) ^{44}Ca with an areal density of 1.83 mg/cm^2. In order to achieve good resolution, we used a relatively thin target foil, because the difference of the atomic energy losses of $^3\mathrm{He}^{2+}$ and the triton in the target causes the energy spread of the outgoing triton. The main contaminant isotope in the target was ^{40}Ca (1.1%).

The outgoing tritons were momentum analyzed within the full acceptance of the spectrometer and detected with a focal-plane detector system that allowed for particle identification and track reconstruction in the horizontal and vertical directions [25]. In the 0° measurement, in addition to tritons, singly charged $^3\mathrm{He}^{1+}$ ions that had captured an electron in the target were also observed at the focal plane. The $^3\mathrm{He}^{1+}$ ions were used to determine the scattering angle "0 degrees" in the acceptance of the Grand Raiden spectrometer, and the relative values of the scattering angle were determined by an angle calibration measurement using a sieve slit. Close to 0°, the scattering angle Θ can be expressed by $\sqrt{\theta^2 + \phi^2}$, where θ and ϕ are the scattering angles in the horizontal and vertical directions, respectively. An angular resolution $\Delta\Theta$ of ≈ 5 mr [full width at half maximum (FWHM)] was achieved by applying the *angular dispersion matching* technique [26] and the "overfocus mode" of the spectrometer [27]. In the analysis, the acceptance of the spectrometer was subdivided into smaller scattering-angle regions in 0.5° steps using the tracking information.

An energy resolution ΔE of 28 keV (FWHM), which is better by a factor of 5 than the energy spread of ≈ 140 keV of the beam, was realized by applying the *lateral dispersion matching* and *focus matching* techniques [26,28]. The "0° spectrum" obtained for the events within the scattering angles $\Theta \leqslant 0.5°$ is shown in Fig. 2 up to $E_x = 16$ MeV. We measured the spectrum up to $E_x = 28$ MeV, but no prominent peak was observed above 14 MeV.

The most strongly excited peak in the spectrum is at ≈ 0.7 MeV. Among the low-lying states of ^{44}Sc with well established J^π values and listed in Ref. [29], this peak was easily identified as the $J^\pi = 1^+$, 0.667 MeV GT state. The second strongest peak was identified as the 0^+, 2.779 MeV state. This state is the IAS of the ground state (g.s.) of ^{44}Ca [29]. On the other hand, most states populated in transitions with $\Delta L \geqslant 1$ were weakly excited at 0°. We see that the $(^3\mathrm{He}, t)$ reaction at forward angles including 0° and at the incoming energy of 140 MeV/nucleon is well suited to study GT states and the IAS populated in $\Delta L = 0$ transitions.

The high energy-resolution of $\Delta E = 28$ keV was essential in separating the IAS and many GT states. With one order-of-magnitude better resolution than in the pioneering ^{44}Ca$(p, n)^{44}$Sc reaction [6], we can now study individual transitions to the IAS and GT states. In ^{44}Sc, the proton separation energy S_p is 6.70 MeV. However, we could see sharp peaks even in the high excitation energy region of the spectrum,

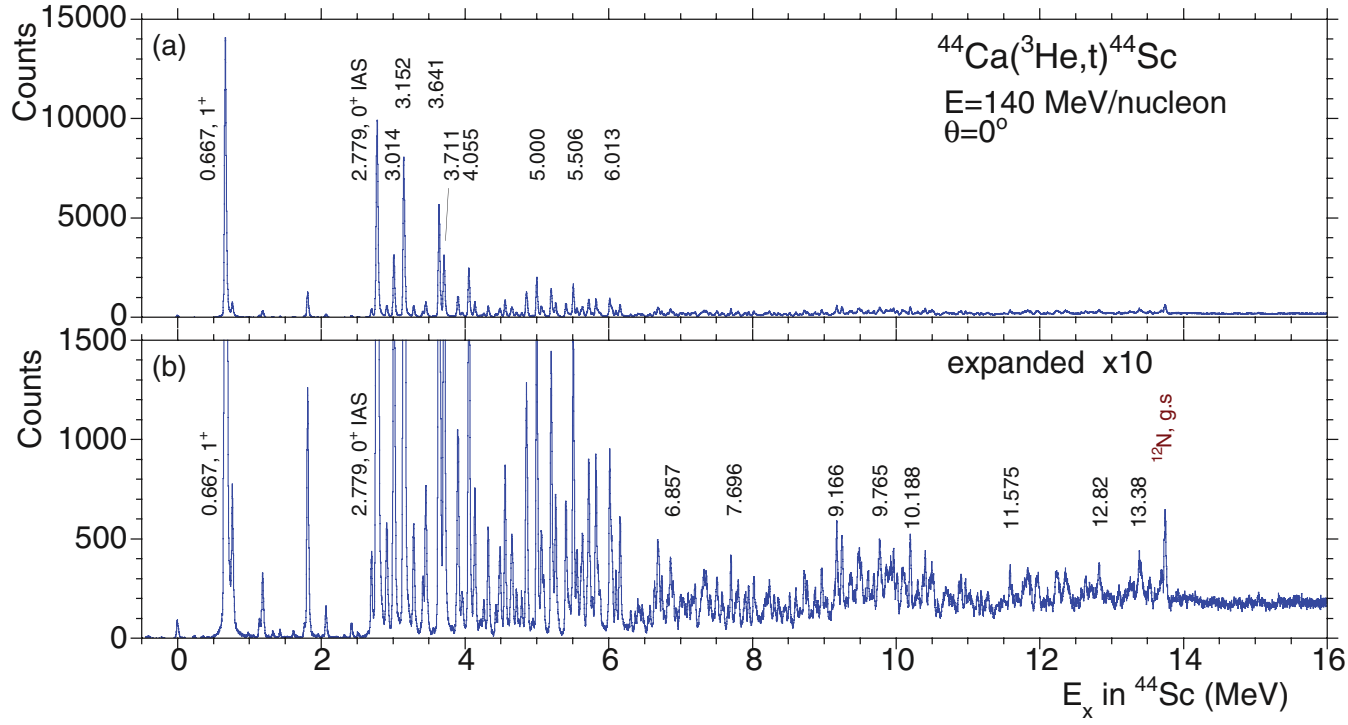

FIG. 2. (Color online) The 0°, ^{44}Ca(^{3}He, t)^{44}Sc spectrum on two scales. The events within the range of scattering angles $\Theta \leqslant 0.5°$ are included. (a) The full count range spectrum. Prominent peaks are observed mainly in the region below 6 MeV. Most of them are populated in $\Delta L = 0$ transitions. (b) The vertical scale is magnified by one order of magnitude, and a fine structure of many states is observed up to $E_x = 14$ MeV. Major states populated in $\Delta L = 0$ transitions are indicated by their excitation energies in MeV.

because the Coulomb barrier and centrifugal potential for an f-shell nucleon are rather large. They are approximately 6 and 8 MeV, respectively.

III. DATA ANALYSIS

The acceptance of the 0° setting and also of the 2.5° setting of the spectrometer was subdivided by a software analysis into five angle cuts of $\Theta \leqslant 0.5°$, 0.5°–1.0°, 1.0°–1.5°, 1.5°–2.0°, and 2.0°–2.5°. The positions and intensities of peaks were obtained up to $E_x = 13.7$ MeV by applying a peak-decomposition program using the shape of the well separated peak at 0.667 MeV as a reference. Since the right tail of this state overlaps with the weak 0.762-MeV state (see Fig. 2), this tail part of the response function was borrowed from the peak shape of the 0.611-MeV state in ^{42}Sc observed in the ^{42}Ca(^{3}He, t)^{42}Sc spectrum taken under the same conditions as the present ^{44}Ca(^{3}He, t)^{44}Sc spectrum.

Above the proton separation energy S_p of 6.70 MeV, a continuum caused by quasifree scattering (QFS) reactions appears. Accordingly, above $E_x \approx 6.7$ MeV, the continuous counts apparently increase with the excitation energy [see Fig. 2(b)]. Therefore, a smooth empirical background connecting the deepest valleys between peaks was subtracted in the peak-fit analysis.

A. Excitation energy

As shown in Table I, only a few GT states are known in ^{44}Sc [29]. Therefore, the E_x values of higher excited states were determined from their peak positions in the $\Theta \leqslant 0.5°$ spectrum with the help of kinematic calculations. The relationship between the peak positions in the spectrum and the corresponding values of magnetic rigidity of the spectrometer was determined using well known E_x values of states in ^{26}Al and ^{24}Al and the peak positions of these states in the spectrum for a natural magnesium (^{nat}Mg) target. The ^{nat}Mg target foil was thin (≈ 1.5 mg/cm^2) and the spectrum was taken under the same experimental conditions as for the ^{44}Ca target.

The reaction Q values in the (^{3}He, t) measurements for the isotopes ^{26}Mg and ^{24}Mg are -4.0 and -13.9 MeV, respectively, and that of ^{44}Ca(^{3}He, t) is -3.7 MeV. The E_x values of ^{26}Al states up to 7.8 MeV are well known. The E_x values of a few low-lying states in ^{24}Al up to 1.09 MeV are also well known. The E_x values of higher excited states in ^{24}Al were determined in a recent β^+-decay study of ^{24}Si [30], although the uncertainties were larger. Therefore, all E_x values of ^{44}Sc states up to $E_x = 14$ MeV listed in Tables I–VI could be determined by interpolation. We estimate that the uncertainties are $\leqslant 4$ keV in the low-lying region up to ≈ 8.1 MeV in ^{44}Sc, and $\leqslant 6$ keV in the region up to ≈ 11.3 MeV for the well isolated peaks with good statistics. For the states in the region between 11.3 and 12 MeV, we estimate larger uncertainties of 10–15 keV. In addition, in the region above $E_x > 12$ MeV, the level density is high, the peaks are overlapping, and thus the peak-decomposition analysis was more difficult. However, since the g.s. excitation energy (i.e., $E_x = 0.0$ MeV) of ^{12}N from the ^{12}C contaminant seen at 13.73 MeV in the ^{44}Sc spectrum [see Fig. 2(b)]

TABLE I. States in ^{44}Sc evaluated in Ref. [29] and observed in the ^{44}Ca(^{3}He, t)^{44}Sc reaction up to $E_x = 4.4$ MeV. The uncertainties for evaluated E_x values (the first column) are given in the cases where they are greater than 1 keV. Unclear uncertainties are indicated by the label (-). Experimental E_x values of close multiplet states can have larger uncertainties than the values mentioned in the text. Less accurate E_x values are indicted by parentheses. Less accurate ΔL values are indicated by parentheses. Observed counts of states in the angle range 0°–0.5° are shown as "Counts (0°)." The B(GT) values are given for the states populated in $\Delta L = 0$ transitions.

Evaluated values[a]		(^{3}He, t)[b]			
E_x (MeV)	J^π	E_x (MeV)	ΔL	Counts (0°)	B(GT)
0.000	2^+	0.0	$\geqslant 1$	1009 (51)	
0.235	2^-	0.236	$\geqslant 1$	76 (18)	
0.667	1^+	0.667	0	182999 (752)	0.714 (36)
0.762	3^+	0.765	$\geqslant 1$	8032 (182)	
0.986	3^+	0.986	$\geqslant 1$	251 (33)	
1.142(5)	1^+	1.143	$\geqslant 1$	1181 (69)	
1.185	3^+	1.187	$\geqslant 1$	3964 (116)	
1.326	3^+	1.330	$\geqslant 1$	338 (36)	
1.426	2^-	1.428	$\geqslant 1$	356 (36)	
1.769	$(2^-, 4^-)$	1.770	$\geqslant 1$	835 (64)	
1.811(2)	$(1, 3)^+$	1.814	0	15114 (219)	0.059 (3)
1.957(5)	$(2–5)^+$	1.959	$\geqslant 1$	133 (28)	
		2.069	0	1667 (101)	0.007 (1)
2.424(2)	$(2–5)^+$	2.426	$\geqslant 1$	783 (70)	
		2.516	$\geqslant 1$	308 (46)	
2.703(3)		2.702	$\geqslant 1$	5249 (185)	
2.779(3)	0^+, IAS	2.779	0	130172 (859)	
2.916(3)	$(2, 3)^+$	2.915	$\geqslant 1$	7167 (218)	
		3.014	0	39126 (479)	0.154 (8)
		3.081	$\geqslant 1$	524 (101)	
3.162(10)	$^+$	3.152	0	98834 (750)	0.390 (20)
3.208(7)		3.221	$\geqslant 1$		
3.285(10)	$(2^+–5^+)$	3.289	(0)	6989 (224)	0.028 (2)
3.323(15)		3.326	$\geqslant 1$	335 (100)	
3.420(11)	$(2^+–5^+)$	3.419	(0)	3616 (179)	0.014 (1)
		3.458	0	9931 (255)	0.039 (2)
		3.557	$\geqslant 1$	557 (43)	
		3.641	0	69055 (400)	0.274 (14)
3.720(-)	$^+$	3.711	0	37404 (299)	0.148 (8)
		3.826	$\geqslant 1$	356 (45)	
3.900(-)	$(^+)$	3.905	0	13002 (227)	0.052 (3)
		(3.956)	$\geqslant 1$	1620 (320)	
		(3.973)	$\geqslant 1$	1489 (326)	
4.053(15)		4.055	0	29956 (268)	0.119 (6)
4.144(10)	$^+$	4.139	$\geqslant 1$	8834 (236)	
		4.261	0	1618 (470)	0.006 (2)
		4.323	0	6536 (158)	0.026 (1)

[a]From Ref. [29].
[b]Present work.

was reproduced with a deviation of 16 keV, we estimate an uncertainty of less than 20 keV even at $E_x = 13.7$ MeV where we stopped the peak-decomposition analysis. Above this energy, as mentioned, no sharp peaks were observed.

B. Assignment of angular momentum transfer ΔL

Gamow-Teller states populated in $\Delta L = 0$ transitions have an angular distribution peaked at 0°. They were distinguished by the decreasing relative peak intensities in the spectra with increasing angle cuts mentioned above, where the relative peak intensities of the prominent 0.667-MeV, 1^+ state in different angle cuts were used as a standard. States with spin-parity assignments of 2^- or 2^+ in Ref. [29] could be easily recognized to have $\Delta L \geqslant 1$ character by the rapid increase of the relative intensities in the spectra with increasing angle cuts. On the other hand, several low-lying states with an assignment of 3^+ in Ref. [29] (states at 0.762, 0.986, 1.185, and 1.326 MeV)

TABLE II. States observed in the ^{44}Ca(^{3}He, t)^{44}Sc reaction between $E_x = 4.4$ and 6.5 MeV. The E_x values obtained for close multiplet states can have larger uncertainties than the values mentioned in the text. Less accurate E_x values are indicted by parentheses. Less accurate ΔL values are indicated by parentheses. Observed counts of states in the angle range 0°–0.5° are shown as "Counts (0°)." The B(GT) values are given for the states populated in $\Delta L = 0$ transitions.

(^{3}He, t)			
E_x (MeV)	ΔL	Counts (0°)	B(GT)
4.430	⩾1	1947 (72)	
(4.470)	⩾1	2053 (205)	
(4.490)	⩾1	4692 (226)	
4.558	0	10357 (152)	0.041 (2)
(4.641)	0	2653 (352)	0.011 (2)
(4.658)	0	4833 (373)	0.019 (2)
4.718	⩾1	2687 (89)	
4.791	0	2365 (83)	0.009 (1)
(4.832)	⩾1	490 (131)	
4.857	0	15515 (223)	0.062 (3)
5.000	0	23328 (222)	0.093 (5)
5.065	0	5921 (143)	0.024 (1)
5.096	0	2614 (116)	0.010 (1)
5.200	0	16332 (238)	0.066 (3)
5.262	0	8148 (160)	0.033 (2)
5.295	⩾1	459 (79)	
5.404	0	8717 (157)	0.035 (2)
(5.439)	⩾1	1416 (131)	
(5.463)	⩾1	1195 (129)	
5.506	0	18625 (203)	0.075 (4)
5.559	0	5029 (118)	0.020 (1)
(5.612)	⩾1	2969 (170)	
5.636	0	5607 (188)	0.023 (1)
(5.700)	0	2462 (184)	0.010 (1)
5.724	0	10582 (226)	0.043 (2)
5.774	(0)	1931 (84)	0.008 (1)
5.822	0	10564 (185)	0.043 (2)
(5.854)	(0)	2459 (145)	0.010 (1)
5.880	0	1779 (134)	0.007 (1)
5.926	⩾1	318 (49)	
5.980	⩾1	561 (75)	
6.013	0	11025 (194)	0.045 (2)
(6.043)	0	4441 (160)	0.018 (1)
6.099	⩾1	3537 (98)	
6.156	0	7289 (131)	0.030 (2)
6.201	⩾1	368 (57)	
6.246	⩾1	362 (47)	
6.303	⩾1	1206 (62)	
6.367	⩾1	966 (65)	
6.404	0	1592 (115)	0.006 (1)
(6.429)	0	1155 (109)	0.005 (1)
6.464	0	1347 (93)	0.005 (1)

TABLE III. States observed in the ^{44}Ca(^{3}He, t)^{44}Sc reaction between $E_x = 6.5$ and 8.5 MeV. For details, see the caption to Table II.

(^{3}He, t)			
E_x (MeV)	ΔL	Counts (0°)	B(GT)
6.547	⩾1	555 (75)	
6.574	⩾1	1366 (87)	
6.635	0	3054 (94)	0.012 (1)
(6.678)	0	4350 (359)	0.018 (2)
(6.696)	0	3310 (354)	0.013 (2)
6.737	0	3026 (103)	0.012 (1)
6.776	0	777 (70)	0.003 (1)
6.818	0	2218 (88)	0.009 (1)
6.857	0	5031 (124)	0.021 (1)
6.893	0	2633 (101)	0.011 (1)
6.990	⩾1	1985 (187)	
7.038	0	1781 (135)	0.007 (1)
(7.068)	0	1095 (92)	0.004 (1)
7.104	0	2288 (90)	0.009 (1)
7.150	0	1883 (191)	0.008 (1)
(7.171)	0	1257 (164)	0.005 (1)
7.198	0	2507 (139)	0.010 (1)
(7.265)	(0)	1161 (113)	0.005 (1)
(7.291)	⩾1	2360 (127)	
7.321	⩾1	3375 (141)	
7.351	(0)	3119 (192)	0.013 (1)
(7.374)	⩾1	932 (182)	
7.407	0	1944 (144)	0.008 (1)
(7.494)	0	2673 (222)	0.011 (1)
(7.514)	0	1585 (237)	0.007 (1)
7.568	0	1967 (108)	0.008 (1)
7.595	0	1047 (100)	0.004 (1)
7.654	(0)	1252 (65)	0.005 (1)
7.696	0	4383 (99)	0.018 (1)
(7.763)	⩾1	2051 (85)	
7.797	0	2964 (95)	0.012 (1)
(7.873)	(0)	967 (121)	0.004 (1)
7.896	⩾1	1914 (127)	
7.942	0	2434 (82)	0.010 (1)
8.016	0	3235 (184)	0.013 (1)
(8.051)	(0)	1143 (79)	0.005 (1)
8.164	⩾1	1666 (95)	
8.193	⩾1	1789 (97)	
8.230	0	2875 (115)	0.012(1)
8.296	⩾1	1908 (135)	
8.356	⩾1	1739 (94)	
(8.385)	⩾1	703 (84)	
8.428	0	1160 (85)	0.005 (1)
8.458	⩾1	1196 (93)	
8.510	0	1974 (142)	0.008 (1)

showed similar relative intensities to 1^+ states in the three small angle cuts of $\Theta \leqslant 0.5°$, 0.5°–1.0°, and 1.0°–1.5°. The increase in the ratio became apparent only in the 1.5°–2.0° cut. Therefore, the spectrum of the 2.0°–2.5° cut derived from the measurement in the 2.5° setting of the spectrometer was useful to distinguish 3^+ states from 1^+ states. Among the states that are clear in the 0.0°–0.5° angle cut and for which no definite J^π values are given in Ref. [29], we found that the states at 2.703, 2.916, and 4.144 MeV are the candidates for 3^+ states from such angular distribution analyses up to 2.5°. The results of the ΔL assignments are listed in Tables I–VI.

Most of the prominent states in the $E_x < 6$ MeV region in the 0.0°–0.5° angle cut shown in Fig. 2 were identified

TABLE IV. States observed in the ^{44}Ca(^{3}He, t)^{44}Sc reaction between $E_x = 8.5$ and 10.2 MeV. For details, see the caption to Table II.

(^{3}He, t)			
E_x (MeV)	ΔL	Counts (0°)	B(GT)
8.594	(0)	2174 (120)	0.009 (1)
8.657	(0)	1012 (94)	0.004 (1)
8.715	0	3684 (114)	0.015 (1)
8.754	0	2317 (286)	0.010 (1)
8.812	(0)	826 (71)	0.003 (1)
(8.848)	(0)	921 (206)	0.004 (1)
(8.862)	(0)	2200 (213)	0.008 (1)
8.906	0	1144 (77)	0.005 (1)
(8.945)	$\geqslant$1	990 (659)	
8.960	(0)	3211 (588)	0.013 (3)
9.010	0	1310 (159)	0.006 (1)
9.035	0	1262 (143)	0.005 (1)
9.101	(0)	1184 (87)	0.005 (1)
9.134	0	1858 (106)	0.008 (1)
9.166	0	6308 (148)	0.027 (1)
9.199	$\geqslant$1	1307 (105)	
9.239	0	5960 (160)	0.025 (2)
9.307	(0)	1526 (104)	0.007 (1)
(9.343)	(0)	2379 (388)	0.010 (2)
(9.363)	(0)	1618 (402)	0.007 (2)
9.381	(0)	1818 (526)	0.008(2)
9.411	$\geqslant$1	1630 (135)	
9.439	$\geqslant$1	1526 (182)	
(9.463)	0	3801 (226)	0.016 (1)
(9.487)	0	3101 (235)	0.013 (1)
9.516	0	2958 (143)	0.013 (1)
9.561	$\geqslant$1	1838 (88)	
9.600	0	3351 (126)	0.014 (1)
(9.631)	$\geqslant$1	984 (184)	
(9.653)	(0)	1476 (189)	0.006(1)
9.683	0	2780 (119)	0.012 (1)
9.735	$\geqslant$1	2964 (125)	
9.765	0	5172 (147)	0.022 (1)
9.798	0	2174 (115)	0.009 (1)
(9.836)	0	2083 (161)	0.009 (1)
(9.860)	0	3258 (165)	0.014 (1)
(9.892)	0	2649 (139)	0.011 (1)
(9.920)	0	3479 (143)	0.015 (1)
9.956	$\geqslant$1	3992 (160)	
(9.984)	$\geqslant$1	966 (172)	
10.007	0	2610 (202)	0.011 (1)
(10.075)	0	2531 (492)	0.011 (2)
(10.094)	0	1615 (445)	0.007 (2)
(10.112)	0	1808 (563)	0.008 (2)
(10.140)	0	1608 (142)	0.007 (1)
10.188	0	5574 (121)	0.024 (1)

TABLE V. States observed in the ^{44}Ca(^{3}He, t)^{44}Sc reaction between $E_x = 10.2$ and 11.3 MeV. For details, see the caption to Table II.

(^{3}He, t)			
E_x (MeV)	ΔL	Counts (0°)	B(GT)
(10.235)	$\geqslant$1	777 (99)	
(10.263)	$\geqslant$1	1334 (109)	
10.294	0	2497 (116)	0.011 (1)
10.364	0	2667 (112)	0.011 (1)
10.397	0	3911 (124)	0.017 (1)
10.455	$\geqslant$1	2164 (333)	
10.487	(0)	2772 (145)	0.012 (1)
(10.514)	$\geqslant$1	2099 (142)	
10.573		1026 (74)	
(10.653)	$\geqslant$1	1301 (115)	
(10.682)	$\geqslant$1	1788 (105)	
(10.712)		1539 (94)	
10.749		1312 (86)	
(10.781)		972 (159)	
(10.803)		624 (156)	
10.865	(0)	2192 (97)	0.010 (1)
10.897	(0)	2401 (94)	0.010 (1)
10.954	(0)	2303 (83)	0.010 (1)
(10.993)	$\geqslant$1	1272 (91)	
(11.023)	$\geqslant$1	1400 (97)	
(11.052)	$\geqslant$1	875 (87)	
11.174	$\geqslant$1	1265 (70)	
(11.251)	$\geqslant$1	872 (151)	
(11.273)	$\geqslant$1	1152 (177)	
11.319	$\geqslant$1	504 (62)	

as $\Delta L = 0$. On the other hand, most of the states enhanced at larger angles and identified as $\Delta L \geqslant 1$ were only weakly excited in the 0.0°–0.5° angle cut. We see that the (^{3}He, t) reaction at 140 MeV/nucleon has a strong selectivity for $\Delta L = 0$ excitations in the measurement at 0°.

The $\Delta L = 0$ assignment was less certain for weakly excited states as well as for multiplets of states, especially for those in the higher E_x region. They are indicated by the label "(0)" in Tables I–VI. In particular, above 12 MeV, the level density becomes high and some states seemed to be doublets or higher multiplets. Since a clear separation of such states was difficult, only candidates for states populated with $\Delta L = 0$ character are listed in Table VI. As will be discussed in Sec. IV C, for most of these states corresponding states were observed in the ^{44}Ca(p, p') experiment performed at 0° and $E_p = 200$ MeV. In (p, p') experiments performed under these conditions, spin-$M1$ states, the analog states of GT states that are excited by the $\Delta L = 0$ and $\Delta S = 1$ transitions, are prominent. Therefore, it is suggested that the $\Delta L = 0$ assignments for these GT states are reasonable.

The 2.779 MeV peak assigned as the IAS of the g.s. of ^{44}Ca [29] also showed a clear $\Delta L = 0$ character. It is expected that the Fermi strength is concentrated in the transition to this IAS. Accordingly, we assume that the states populated in $\Delta L = 0$ transitions, except the IAS, are GT states [4].

C. Gamow-Teller transition strength

The reduced GT transition strength B(GT) can be derived for each of the GT states using the proportionality given by Eq. (2). In order to evaluate the E_x dependence of $F(q, \omega)$ in Eq. (2), a DWBA calculation was performed for the ^{44}Ca(^{3}He, t)^{44}Sc reaction using the computer code DW81

TABLE VI. States observed in the ^{44}Ca(^{3}He, t)^{44}Sc reaction between $E_x = 11.3$ and 13.7 MeV. The E_x values of close multiplet states can have larger uncertainties than the values mentioned in the text. Less accurate E_x values are indicted by parentheses. Less accurate assignments of ΔL values are indicted by parentheses. Observed counts of states in the angle range 0°–0.5° are shown as "Counts (0°)." The B(GT) values are given for the states populated in $\Delta L = 0$ transitions. In the region above 12 MeV, complete separation of states was difficult. Therefore, only the candidates states populated in $\Delta L = 0$ transitions are listed. For the states in the region above 11.5 MeV, values of isospin T can be suggested (see text). These T values are given in the last column.

		(^{3}He, t)		
E_x (MeV)	ΔL	Counts (0°)	B(GT)	T
(11.383)	$\geqslant$1	721 (74)		
(11.415)	$\geqslant$1	754 (76)		
11.455	$\geqslant$1	767 (76)		
11.489	$\geqslant$1	1168 (100)		
11.575	(0)	3022 (109)	0.013 (1)	(2)
(11.611)	$\geqslant$1	1383 (83)		
(11.656)	$\geqslant$1	1149 (105)		
(11.683)		915 (103)		
11.750	(0)	1701 (93)	0.008 (1)	2
(11.783)	(0)	2105 (110)	0.009 (1)	2
(11.815)	$\geqslant$1	2089 (245)		
(11.836)	$\geqslant$1	1835 (226)		
(11.865)	(0)	1722 (243)	0.008 (1)	(2)
(11.931)	(0)	1828 (157)	0.008 (1)	(2)
(11.956)	$\geqslant$1	1771 (160)		
(11.979)		1396 (171)		
12.10	(0)	1194 (82)	0.005 (1)	
12.56	(0)	1143 (131)	0.005(1)	(2)
12.63	(0)	2172 (107)	0.010 (1)	2
12.82	(0)	2688 (173)	0.012(1)	1
13.10	(0)	1353 (101)	0.006 (1)	(2)
13.38	(0)	4998 (320)	0.023 (2)	2
13.53	(0)	2042 (250)	0.009 (1)	2
13.68	(0)	3149 (210)	0.014(1)	2
13.732[a]				

[a]The ground state of ^{12}N.

[31] following the procedure discussed in Refs. [32–34]. The optical potential parameters were taken from Ref. [35]. We considered two possible shell-model (SM) configurations of $(\pi f_{7/2}, \nu f_{7/2}^{-1})$ and $(\pi f_{5/2}, \nu f_{7/2}^{-1})$ in the final nucleus ^{44}Sc. The calculations show that $F(q, \omega)$ decreases gradually with excitation energy. The amount of decrease was about 3.5% at $E_x =$ 6.0 MeV and 12% at 12.0 MeV. In addition, for both of the SM configurations, the amount of decrease was very similar.

In order to use Eq. (2), we need the value of $\hat{\sigma}^{\mathrm{GT}}$. For this purpose, we introduce the ratio of GT and Fermi unit cross sections denoted as R^2 [7] and defined by

$$R^2 = \frac{\hat{\sigma}^{\mathrm{GT}}}{\hat{\sigma}^{\mathrm{F}}} = \frac{\sigma^{\mathrm{GT}}(0)}{B(\mathrm{GT})} \Big/ \frac{\sigma^{\mathrm{F}}(0)}{B(\mathrm{F})}, \tag{3}$$

where $\sigma^{\mathrm{GT}}(0)$ and $\sigma^{\mathrm{F}}(0)$ are the GT and Fermi cross sections at $q = \omega = 0$ after making the DWBA corrections, respectively, and $\hat{\sigma}^{\mathrm{F}}$ is the unit Fermi cross section defined by $\sigma^{\mathrm{F}}(0)/B(F)$. We assume that all of the Fermi transition strength is concentrated in the IAS and consumes the complete sum rule value of $B(\mathrm{F}) = N - Z = 4$. We also assume that R^2 is a smooth function of A. Therefore, once the R^2 value is obtained for mass $A = 44$ nuclei, $\hat{\sigma}^{\mathrm{GT}}$ is known using the $\sigma^{\mathrm{F}}(0)$ value of the IAS that can be derived experimentally.

The A dependence of R^2 was systematically studied, and a smooth increase in R^2 was observed with increasing A [36,37]. A value of 7.8 ± 0.4 can be deduced for the $A = 44$ nuclei by quadratically interpolating the experimentally obtained R^2 values for $A = 26$ [13], 34 [16], 46 [38], 54 [9], 64 [39], 78 [40], 118, and 120 [41]. Using the obtained R^2 value, the B(GT) value for each GT excitation is calculated. They are listed for all states with $\Delta L = 0$ character in Tables I–VI.

The uncertainty of B(GT) value includes the uncertainty of the experimental count for each state in the "0° spectrum" [see the column "Counts (0°)" of Tables I–VI] that includes the statistical uncertainty and the uncertainties in the peak-decomposition analysis. The ≈5% uncertainty in the R^2 value is also added. However, possible contributions of the tensor interaction are not included. The contributions are usually small, but can be large for weakly excited states (for example, see the discussion in Ref. [16]). In addition, the uncertainties associated with the subtraction of the QFS continuum were not included. Therefore, the B(GT) values of the states in the region above $E_x \approx 9$ MeV, where the continuous counts were getting larger, can have larger uncertainties than are indicated.

As discussed in Sec. I B, the studies of the ^{44}Ca(^{3}He, t)^{44}Sc, CE reaction and the β decay of ^{44}Cr provide information on mirror GT transitions, and the B(GT) values of the mirror GT transitions are identical under the assumption of isospin symmetry. It should be noted that the half-life in a β decay is largely dependent on the distribution of GT transition strength as a function of excitation energy in the final nucleus. As will be discussed in Sec. IV B1, the β-decay half-life of ^{44}Cr can be reproduced using the Fermi strength and the GT strength distribution given in the tables. This indicates that the gross features of the B(GT) distribution obtained here are similar to those in the ^{44}Cr β decay, and thus, the obtained B(GT) values are reasonable.

As mentioned, the main contaminant isotope in the target was ^{40}Ca (1.1%). To identify the ^{40}Sc states in the ^{44}Sc spectrum, if any, we recorded the 0°, (^{3}He, t) spectrum from an enriched ^{40}Ca target under the same experimental conditions as for the ^{44}Ca target. However, no state corresponding to the excitation of ^{40}Sc states was observed in the ^{44}Sc spectrum. The ^{40}Ca(p, n)^{40}Sc reaction at $E_p = 160$ MeV was performed at the Indiana University Cyclotron Facility (IUCF) [42]. They reported that the strongest GT state is at 2.75 MeV in ^{40}Sc. Due to the difference of the reaction Q values, this state is expected at $E_x = 13.42$ MeV in the ^{44}Sc spectrum. The reported B(GT) value for the transition to this state was 0.21(4). Taking the small ^{40}Ca abundance of 1.1% in the target into account, the expected strength corresponds to the B(GT) value of ≈ 0.002 in the ^{44}Sc spectrum. This value is smaller than our sensitivity limit of B(GT) ≈ 0.005.

IV. DISCUSSION

A. Gamow-Teller strength distribution

The B(GT) distribution obtained in the experiment is shown in Fig. 3(a). The main part of the strength is concentrated in the region below $E_x = 6$ MeV. Above this energy, the B(GT) strengths were weak and terminate at 13.7 MeV. They are in agreement with the features of the 0° spectrum obtained in the ^{44}Ca$(p, n)^{44}$Sc reaction at $E_p = 120$ MeV and shown in Ref. [6]. A large difference, however, is due to our one order-of-magnitude better resolution; we see that the strength is highly fragmented. In addition, the GT states and the IAS were separated, and thus reliable excitation strengths were obtained separately for these states.

The B(GT) distribution from a SM calculation is shown in Fig. 3(b). The SM calculation was performed using the GXPF1J interaction [43,44]. The model space was restricted to the pf-shell and an inert ^{40}Ca core was assumed. The B(GT) values shown include the quenching factor of $(0.74)^2$. The SM calculation reproduces the concentration of the B(GT) strength in the region up to $E_x = 6$ MeV, but not the fragmentation of the strength. It is suggested that the fragmentation in this region is caused by the contribution of the intruder sd-shell configurations that are not included in the calculation.

The experimental and SM cumulative sums (CS) up to 14.0 MeV are shown in Fig. 4. The agreement is rather good up to $E_x = 4$ MeV, but the SM CS values are much larger than the experimental CS values above 5 MeV. The total CS value of the B(GT) strength experimentally observed in the transition to discrete states was 3.72. Although we suggest that this experimental CS value is the minimum of the total sum in the entire region up to $E_x = 14$ MeV, the value of 5.75 from the SM calculation in the same region is about 50% larger.

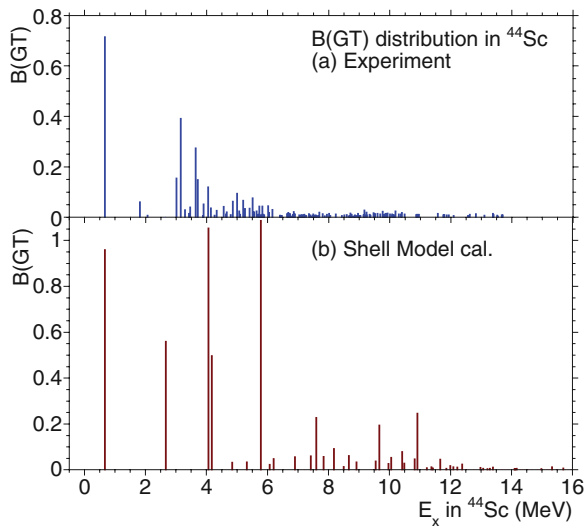

FIG. 3. (Color online) A comparison of the experimental and theoretical B(GT) strength distributions with (a) the B(GT) strength distribution derived from the ^{44}Ca$(^3$He$, t)$ measurement, and (b) the B(GT) strength distribution from the shell model (SM) calculation using the effective interaction GXPF1J. A quenching factor of $(0.74)^2$ is included.

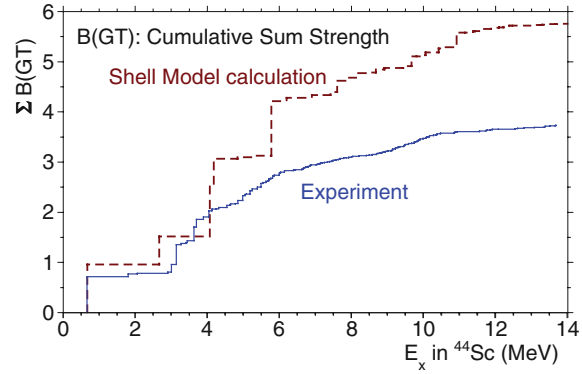

FIG. 4. (Color online) A comparison of the cumulative sums (CSs) of B(GT) strengths from the experimental ^{44}Ca$(^3$He$, t)$ measurement and the SM calculation using the effective interaction GXPF1J. A quenching factor of $(0.74)^2$ is included in the SM calculation.

Above $E_x = 6.2$ MeV, the experimentally observed states are only weakly populated and most of them have B(GT) $<$ 0.02. Therefore, the first saturation (or the plateau) of the experimental CS strength is observed at 6.2 MeV. This saturation at $E_x \approx 6$ MeV is reproduced in the SM calculation.

The continuum caused by the QFS can appear above $S_p = 6.70$ MeV. Since there is no theory for reliably calculating the cross section of the QFS continuum, a background described by a smooth line was subtracted in our analysis, as mentioned above (see also discussions in Refs. [45,46]). Accordingly B(GT) strengths in the continuum, if any, are not included in the summed B(GT) strength. In order to get the maximum B(GT) strength in the continuum, we evaluated the B(GT) strength under the extreme assumption that all continuum counts are due to GT transitions. The result suggested that they would add additional B(GT) strength of 1.17 to the summed B(GT) strength in the region up to 14 MeV.

The Ikeda sum rule for GT strengths in nuclei is expressed as $\Sigma B(\mathrm{GT}_-) - \Sigma B(\mathrm{GT}_+) = 3(N - Z)$, where $\Sigma B(\mathrm{GT}_-)$ and $\Sigma B(\mathrm{GT}_+)$ are sums of GT$_-$ and GT$_+$ transition strengths measured by (p, n)- and (n, p)-type reactions [2,47]. Since the excess of neutrons in the target nucleus ^{44}Ca is 4, the value $3(N - Z)$ is 12. The total sum of the B(GT) strength experimentally observed in the transition to discrete states is 3.72, that is, 31% of 12, and the maximum B(GT) value in the continuum is 1.17. Therefore, the value $\Sigma B(\mathrm{GT}_-)$ up to 14 MeV cannot be more than 4.89. As will be discussed in Sec. IV C, it is expected that the strength $\Sigma B(\mathrm{GT}_+)$, i.e., the strength in the (n, p) direction, is small. Therefore, our result shows that the total sum of the B(GT) strength located in the energy region from 0 to 14 MeV cannot be more than 41% of the sum-rule-limit value.

The analysis for the $T_z = +4 \rightarrow +3$, ^{64}Ni$(^3$He$, t)^{64}$Cu reaction [39] showed that the $\Sigma B(\mathrm{GT}_-)$ strength located in the energy region up to 17 MeV was around 44% of the sum-rule-limit value and cannot be more than 55%. A very general value of $\approx$60% is suggested in the region up to $\approx$15 MeV of excitation from (p, n) measurements [6]. We notice that our $\Sigma B(\mathrm{GT}_-)$ strength is smaller than these values. It is discussed in Ref. [48] that the B(GT$_-$) strength can be

pushed up to ≈50 MeV. It is an interesting question if there is some mechanism that pushes more GT strength higher up out of the energy region of our analysis in the ^{44}Ca →^{44}Sc transition.

B. Comparison with mirror β decay

The ^{44}Ca(^{3}He, t)^{44}Sc reaction provides information on the GT transitions and the Fermi transition with $T_z = +2 \rightarrow +1$, while the β decay of ^{44}Cr to ^{44}V allows the study of the analogous transitions with $T_z = -2 \rightarrow -1$ (see Fig. 1). The isotope ^{44}Cr was first observed at GANIL [49]. In a recent study with higher statistics (number of implantations ≈ 6.76 × 10^4) [21], a delayed-proton spectrum has been measured and a $T_{1/2}$ value of 42.8(6) ms has been obtained.

Assuming isospin symmetry, we first estimate the ^{44}Cr →^{44}V β-decay half-life using the B(GT) distribution derived from the analysis of the ^{44}Ca(^{3}He, t)^{44}Sc measurement. Then, the "β-decay spectrum" is deduced from the ^{44}Ca(^{3}He, t)^{44}Sc spectrum and compared with the delayed-proton spectrum measured in the β-decay study of ^{44}Cr.

1. *Derivation of ^{44}Cr β-decay half-life from the strengths of mirror Fermi and Gamow-Teller transitions*

The β-decay $T_{1/2}$ value depends on how large the contributions of Fermi and GT transitions are in the Q window of the decay. Therefore, the $T_{1/2}$ value of each β decay reflects the specific strength distribution of the GT transitions and the Fermi transition as a function of E_x. Here, we start with the relationship that the inverse of the total half-life $T_{1/2}$ of a β decay can be written using B(F) and B_j(GT) values of the GT transitions to the jth excited states as [4,50]

$$\frac{1}{T_{1/2}} = \frac{1}{K}\left[B(\mathrm{F})f_{\mathrm{F}}(1-\delta_c) + \lambda^2 \sum_{j=\mathrm{GT}} B_j(\mathrm{GT})f_j\right], \quad (4)$$

where δ_c is the Coulomb correction factor having a value less than 0.01 [51] and f_{F} and f_j are the phase-space factors (f factors) for the Fermi and the jth GT transition, respectively. It should be noted that the inverse of the half-life is proportional to the total transition strength in the β decay.

Assuming isospin symmetry, $T_z = \pm 2 \rightarrow \pm 1$, mirror GT transitions should have the same B(GT) values. In addition, E_x values of GT states in the final $T_z = \pm 1$ nuclei should be the same. Then, the half-life $T_{1/2}$ of the ^{44}Cr →^{44}V β decay can be derived by combining the value of B(F) = 4 and the B(GT) values that are obtained from the ^{44}Ca(^{3}He, t)^{44}Sc study with the f factors of the ^{44}Cr β decay. The f factor for each transition can be calculated using the Q_β of the ^{44}Cr β decay and the E_x value of each state determined in the ^{44}Ca(^{3}He, t) study.

The Q_β value of 10.970(230) is given in Ref. [29]. Since the f factor decreases rapidly with E_x [f is approximately proportional to $(Q_\beta - E_x)^5$] [52], the GT transitions to the higher excitation region contribute very little to the $T_{1/2}$ value [see the discussion in Sec. IV B2 and Fig. 5(d)]. Taking the contributions of GT transitions up to 7 MeV into account, a

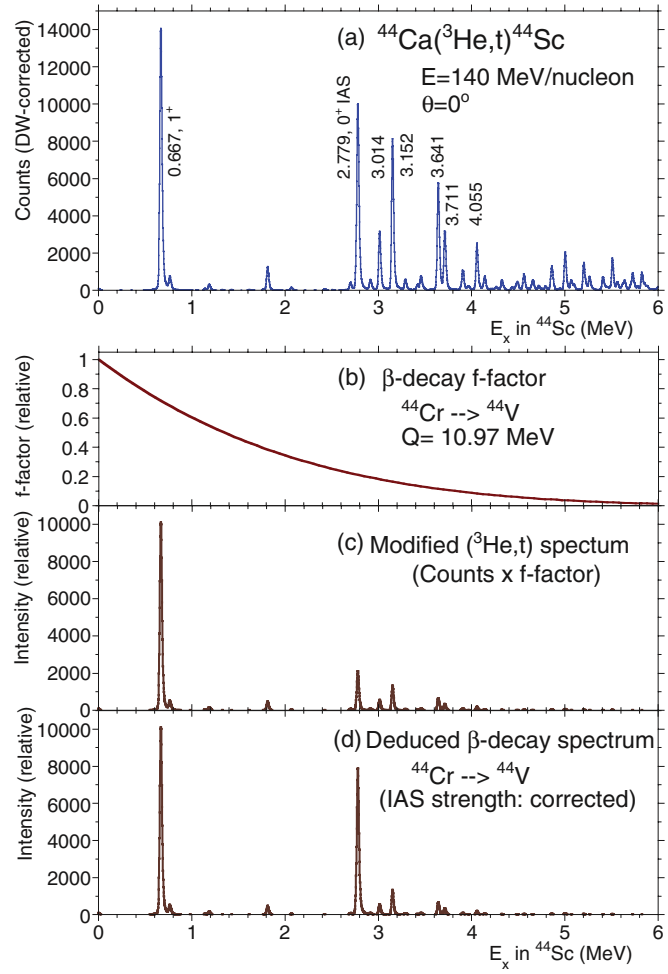

FIG. 5. (Color online) (a) The low-excitation energy region of the ^{44}Ca(^{3}He, t)^{44}Sc spectrum for events with scattering angles Θ ⩽ 0.5°. Major states with $\Delta L = 0$ character are indicated by their excitation energies in MeV. The spectrum has been modified to include the decrease of the cross section caused by the factor $F(q, \omega)$ in Eq. (2). Therefore, the heights of GT states are almost proportional to B(GT) values. (b) The f factor for the ^{44}Cr β decay normalized to unity at $E_x = 0$ MeV. (c) The modified ^{44}Ca(^{3}He, t)^{44}Sc spectrum that is obtained by multiplying the (^{3}He, t) spectrum given in panel (a) with the f factor shown in panel (b). (d) The deduced β-decay spectrum of ^{44}Cr after making the correction of the IAS strength. Note that the IAS is stronger by a factor of R^2/λ^2 in a β decay compared to the corresponding CE reaction (see text).

$T_{1/2}$ value of 40(5) ms was obtained, where f factors were calculated following Ref. [52]. The uncertainty of 15% of the $T_{1/2}$ value is due to large uncertainties in the f factors, that further originated from the large uncertainty of the Q_β value of the ^{44}Cr → ^{44}V β decay. It is noted that our $T_{1/2}$ value was derived using the B(F) and B(GT) strength distribution in the $T_z = +2 \rightarrow +1$ transition. The agreement of the $T_{1/2}$ value of 40(5) ms derived in this "merged analysis" [4,50] with the β-decay value of 42.8(6) ms [21] suggests that the experimentally obtained B(GT) values, especially those for the transitions to the low-lying GT states that make large contributions to the second term of Eq. (4), are reasonable.

2. *Estimation of the* ^{44}Cr → ^{44}V *β-decay spectrum*

The 0°, ^{44}Ca(^{3}He, t)^{44}Sc spectrum up to $E_x = 6$ MeV is shown in Fig. 5(a). The spectrum has been modified to include the correction of the factor $F(q, \omega)$ in Eq. (2) (≈4% decrease at $E_x = 6$ MeV). Therefore, assuming the same peak shape for all GT states prominent in this figure, the heights of peaks are almost proportional to B(GT) values. On the other hand, in the β decay of ^{44}Cr, intensities of the jth GT and Fermi transitions are proportional to the values $B_j(\mathrm{GT})f_j$ and $B(\mathrm{F})f_\mathrm{F}$, respectively [see Eq. (4)]. The f factors normalized to unity at $E_x = 0$ are shown in Fig. 5(b). We see a rapid decrease as a function of E_x.

To estimate the ^{44}Cr "β-decay spectrum" from the ^{44}Ca(^{3}He, t) spectrum under the assumption of isospin symmetry, the ^{44}Ca(^{3}He, t) spectrum was first multiplied by the f factor [see Fig. 5(c)]. This modified spectrum shows that no significant intensity (branching ratio) of GT transitions is expected to the states above $E_x \approx 4.5$ MeV in the β decay of ^{44}Cr.

The 2.779-MeV state is the IAS that carries the Fermi transition strength of $B(\mathrm{F}) = 4$. It should be noted that the ratios of the coupling constants (interaction strengths) for the τ and $\sigma\tau$ operators that cause Fermi and GT transitions, respectively, are different in the ^{44}Ca(^{3}He, t)^{44}Sc reaction and the ^{44}Cr →^{44}V β decay. Therefore, we consider modifying the intensity of the IAS peak in Fig. 5(c) so as to represent the Fermi transition strength in the ^{44}Cr β decay.

In order to understand the difference of the Fermi and GT coupling constants in the β decay and the (^{3}He, t) reaction, we express the B(GT) values and B(F) value in Eq. (4) in terms of the cross sections of GT states and the IAS in the (^{3}He, t) reaction. In the (^{3}He, t) reaction, the cross sections for the Fermi and the jth GT transitions at $q = \omega = 0$ are given by $\sigma^\mathrm{F} = \hat{\sigma}^\mathrm{F} B(\mathrm{F})$ and $\sigma_j^\mathrm{GT} = \hat{\sigma}^\mathrm{GT} B_j(\mathrm{GT})$, respectively, where the ratio of $\hat{\sigma}^\mathrm{GT}$ and $\hat{\sigma}^\mathrm{F}$ is the R^2 value [see Eq. (3)]. Using these values, Eq. (4) can be written as

$$\frac{1}{T_{1/2}} = \frac{1}{K\hat{\sigma}^\mathrm{F}} \frac{\lambda^2}{R^2} \left[\frac{R^2}{\lambda^2} \sigma^\mathrm{F} f_\mathrm{F}(1-\delta_c) + \sum_{j=\mathrm{GT}} \sigma_j^\mathrm{GT} f_j \right]. \quad (5)$$

This relationship shows that the contribution of the term "$\sigma^\mathrm{F} f_\mathrm{F}$" of the Fermi transition to the value $1/T_{1/2}$, i.e., the total β-decay transition strength, is larger by a factor of R^2/λ^2, that is, ≈ 4.9, than the terms "$\sigma_j^\mathrm{GT} f_j$" of the GT transitions, meaning that the IAS peak in the "β decay spectrum" is enhanced by this factor compared to the strength in the modified (^{3}He, t) spectrum shown in Fig. 5(c). The "deduced β-decay spectrum" finally obtained for ^{44}Cr β decay is shown in Fig. 5(d).

3. *Comparison with the delayed-proton spectrum of* ^{44}Cr *β decay*

The delayed-proton spectrum measured in the study of ^{44}Cr β decay [21] is shown in Fig. 6(a). The energy resolution of the proton spectrum was ≈150 keV (FWHM). The proton separation energy S_p in ^{44}V is 2.08 ± 0.12 MeV [29]. It is estimated that the proton emission is much faster than the γ-ray emission at excitation energies about 1 MeV above the S_p in the middle of f-shell nuclei [21]. Assuming direct decay

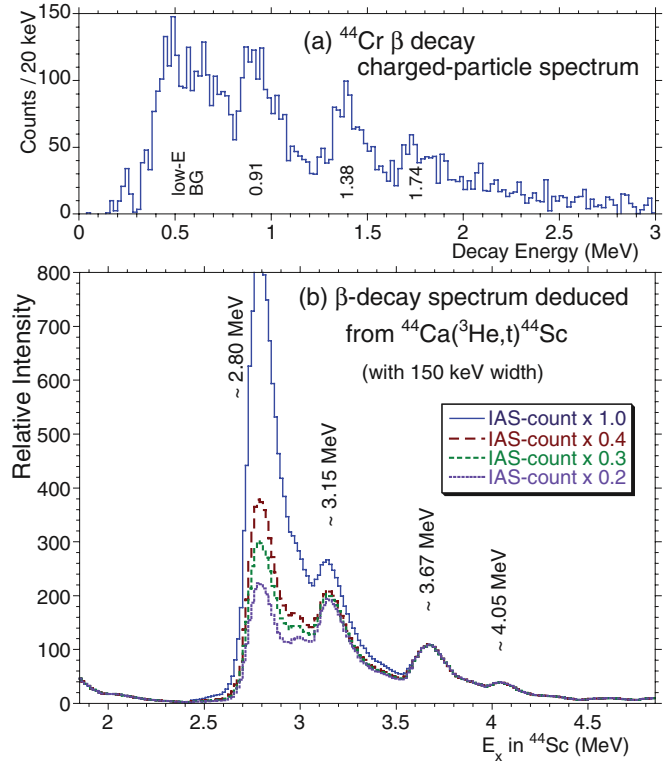

FIG. 6. (Color online) (a) The delayed charged-particle spectrum from the ^{44}Cr β decay [21]. The low-energy bump indicated by "low-E BG" originates in the emission of β^+ particles, while other peaks are from the delayed-proton emission, where the pileup of β-particle energy broadens the peaks and makes the high-energy tails of the peaks wide. The peaks are identified by the energy given in Ref. [21]. The energy resolution (ΔE) is about 150 keV (FWHM). (b) The β-decay spectrum deduced from the ^{44}Ca(^{3}He, t) spectrum. The spectrum shown in Fig. 5(d) was convoluted with the ΔE of 150 keV of the delayed-proton spectrum shown in panel (a). The energy scale is shifted by 1.8 MeV to get a good agreement with the delayed-proton spectrum. The vertical scale is normalized so that the 3.67 MeV peak consisting of a few GT states has approximately the same height as the corresponding 1.74 MeV peak in panel (a). The solid line was obtained by a simple convolution of the 150 keV (FWHM) width. The dashed, short-dashed, and dotted lines were obtained by reducing the IAS strength down to 40%, 30%, and 20%, respectively, in order to simulate the suppression of the proton emission from the IAS.

of protons to the g.s. of ^{43}Ti [21], it is expected that the delayed-proton spectrum represents mostly the "β-decay spectrum."

In order to compare and study the symmetry of the analogous $T_z = \pm 2 \rightarrow \pm 1$, GT and Fermi transitions, the "deduced β-decay spectrum" shown in Fig. 5(d) was given a width of 150 keV corresponding to the resolution of the delayed-proton spectrum. The spectrum obtained is indicated by the solid line in Fig. 6(b), where the energy scale is displaced by 1.8 MeV compared to Fig. 6(a) to get a good agreement in the peak positions. This value is about 0.3 MeV smaller than the S_p of 2.08 MeV in ^{44}V. The vertical scales are adjusted so that the 1.74 MeV peak in the delayed-proton spectrum [Fig. 6(a)] and the 3.67 MeV peak (in reality consisting of a few GT states) in the "deduced β-decay spectrum" derived

from the ^{44}Ca(^{3}He, t) spectrum [Fig. 6(b)] have approximately the same height.

It is clear that the strength of the 0.91 MeV peak in Fig. 6(a), mainly representing the strength of the Fermi transition, is largely suppressed compared to the corresponding 2.80 MeV peak shown by the solid line in Fig. 6(b). We found that the strength ratio of the three main peaks at 0.91, 1.38, and 1.74 MeV in the delayed-proton spectrum [Fig. 6(a)] cannot be reproduced unless the strength of the 2.779 MeV, IAS peak is reduced to $\approx$30% of the original strength in the modified ^{44}Ca(^{3}He, t) spectrum [the short broken line in Fig. 6(b)]. In addition, if the bump structure of the low-energy background ["low-E BG" bump in Fig. 6(a)], caused by the energy deposited by the β^{+} particles, has a high-energy tail that overlaps with the 0.91 MeV peak, the strength of the 2.779 MeV, IAS peak should be further reduced to $\approx$20% [the dotted line in Fig. 6(b)] to achieve a good agreement.

We notice that the decay of the $T = 2$, IAS in the $T_z = -1$ nucleus ^{44}V into a proton having $T_z = -1/2$ and $T = 1/2$ and the ^{43}Ti having $T_z = -1/2$ and the $T = 1/2$ g.s. (and also the $T = 1/2$ low-lying states) is not allowed by the isospin selection rule. If this is the case, it is suggested that the observed proton-decay strength of $\approx$ 20%–30% of the expected full strength was caused by the $T = 1$, isospin impurity components in the "$T = 2$" IAS [20]. In addition, the Coulomb barrier may still hinder the decay of protons with an energy slightly less than 1 MeV. In any case, the remaining $\approx$ 70%–80% of the IAS feeding in the β decay of ^{44}Cr must decay in the form of a β-delayed γ that was not detected in the experiment [21].

The 1.38 MeV peak in the proton-decay spectrum [Fig. 6(a)] is situated about 0.25 MeV higher than the corresponding 3.15 MeV peak in Fig. 6(b). The displacement may be due to isospin asymmetry. For further discussion, however, a delayed-proton spectrum with higher quality is needed.

C. Isospin T of Gamow-Teller states

We discuss the values of isospin T for highly excited GT states by comparing the spectra from our ^{44}Ca(^{3}He, t), CE reaction and the ^{44}Ca(p, p') proton inelastic-scattering measurement performed at 0° and $E_p = 200$ MeV. For this purpose, we first summarize the properties and isospin structure of spin-$M1$ excitations best studied by (p, p') reactions. Then, we discuss their analogous relationship with GT excitations and the identification of the values of isospin T.

1. Properties and the isospin structure of spin-$M1$ excitations

In (p, p') reactions at intermediate energies, spin-$M1$ states excited by $M1_\sigma$ transitions become prominent at 0° [2,53]. These spin-$M1$ states in an even-even nucleus have J^π values of 1^+. If the $M1_\sigma$ transitions start from the 0^+ g.s. of nuclei with the isospin $T = T_0 \geqslant 1$, where T_0 is the T value of the g.s., they are mainly caused by the $\sigma\tau$ operator, because the contribution of the σ operator is much smaller [2,53]. Then, as for GT transitions, we can define the reduced spin-$M1$ transition strength $B(M1_\sigma)$. In addition, we can expect a close proportionality between the cross sections of $M1_\sigma$ excitations and the $B(M1_\sigma)$ values,

$$\sigma^{M1\sigma}(q,\omega) \simeq K(\omega) N_{\sigma\tau} |J_{\sigma\tau}(q)|^2 B(M1_\sigma) \quad (6)$$

$$= \hat{\sigma}^{M1\sigma} F(q,\omega) B(M1_\sigma), \quad (7)$$

where $\hat{\sigma}^{M1\sigma}$ is the unit cross section for the $M1_\sigma$ transition. Owing to the close proportionality in both the (^{3}He, t) and (p, p') reactions, it is expected that the analog GT and spin-$M1$ states are excited with corresponding strengths. Therefore, analogous structures of GT and spin-$M1$ states in ^{44}Sc and ^{44}Ca, respectively, can be studied by comparing the spectra from the ^{44}Ca(^{3}He, t)^{44}Sc and ^{44}Ca(p, p') reactions (see Fig. 1).

The main differences in these reactions are that the (p, p') experiments access the structure in the initial (Z, N) nuclei having $T_z = (N - Z)/2$, whereas the (^{3}He, t) reactions access the structure in the ($Z + 1$, $N - 1$) final nuclei having $T_z = (N - Z)/2 - 1$. Accordingly, as shown in Fig. 1, starting from the $T_z = +2$, $T = T_0 = 2$, $J^\pi = 0^+$ g.s. of ^{44}Ca, the $J^\pi = 1^+$, spin-$M1$ states with $T = T_0 = 2$ and $T_0 + 1 = 3$ are excited by the $\sigma\tau$-type interaction in the ^{44}Ca(p, p') experiment. On the other hand, in the ^{44}Ca(^{3}He, t) reaction, GT states with $T = T_0 - 1 = 1$, $T_0 = 2$, and $T_0 + 1 = 3$ can be excited in the $T_z = +1$ nucleus ^{44}Sc, where higher T states are expected at higher energies due to the isovector and isotensor terms of the symmetry energy [19,54,55], although they can coexist in the transitional region. Therefore, if a corresponding spin-$M1$ state is found for a GT state, the GT state has an isospin value of either $T = 2$ or 3, and if not, it should have $T = 1$. In order to distinguish the $T = 3$ states from the $T = 2$ states, if necessary, we can further use the fact that the squares of the isospin Clebsch-Gordan coefficients (CG^2) in the excitation of these different T states are different for the (^{3}He, t) and (p, p') reactions [4]. We also note that only $T = T_0 + 1 = 3$ states are excited in (n, p)-type (β^{+}-type) CE reactions on the target nucleus ^{44}Ca (see Fig. 1).

In (p, p') measurements for the pf-shell nuclei, it is reported that the spin-$M1$, 1^+ states are mainly observed in the $E_x = 7$–14 MeV region [56–58]. In addition, isospin values of 1^+ states in isobars with the $A = 58$, ^{58}Ni and ^{58}Cu pair and the $A = 54$, ^{54}Fe and ^{54}Co pair were investigated by comparing the spectra obtained in (p, p') and (^{3}He, t) reactions [9,10]. The (p, p') measurements on the $T_z = T_0 = +1$ target nuclei ^{58}Ni and ^{54}Fe were performed at 0° and $E_p = 160$ MeV and the resulting spectra for $E_x > 8.3$ MeV were obtained. The T values were identified on the basis of the different excitation strengths of analog spin-$M1$ and GT states in the (p, p') and (^{3}He, t) reactions due to the differences in the CG^2 values in the feeding of analog GT and spin-$M1$ states with different T values [4]. As a result, it was found that the $T = T_0 = 1$, spin-$M1$ states are located mainly below $E_x = 11$ MeV, while the $T = T_0 + 1 = 2$ states lie between 10 and 13 MeV in these $T_z = T_0 = 1$ nuclei ^{58}Ni and ^{54}Fe.

Taking these observed excitation energies into consideration, we estimate that the $T = T_0 = 2$, spin-$M1$ states are located in the region of $\approx$7–11 MeV in ^{44}Ca, because similar centroid energies are expected [19] for the $T = T_0$, spin-$M1$ excitations with the same main configuration of ($f_{5/2}$, $f_{7/2}^{-1}$). On the other hand, to estimate the excitation energy of the

$T = T_0 + 1 = 3$, spin-$M1$ states, we have to take into account the effect that the $T_0 + 1$ states are pushed up by another $\approx$1.5 MeV by the symmetry energy in the $T_z = T_0 = +2$ nucleus compared to the $T_z = T_0 = +1$ nuclei [19]. Therefore, the $T = 3$, spin-$M1$ states are expected roughly in the 11.5–14.5 MeV region of ^{44}Ca.

2. *Comparison of* ^{44}Ca(^{3}He, t) *and* ^{44}Ca(p, p') *spectra*

In Ref. [59], a ^{44}Ca(p, p') spectrum taken at very forward angles including 0° is presented. The experiment was carried out at IUCF at an incoming proton energy of 200 MeV using the K600 magnetic spectrometer. A self-supporting ^{44}Ca target with an enrichment of 98.68% and an areal density of 3.2(3) mg/cm^2 was used. The transmission mode of the K600 spectrometer, where the incoming proton beam directly passes through the spectrometer, was used in the experiment. As a result, only the region above the threshold energy of 8.3 MeV in ^{44}Ca could be studied. As we see from the spectrum shown in Fig. 7(b), the detection efficiency above the threshold region increases gradually. The energy resolution of $\approx$40 keV (FWHM) achieved in the (p, p') measurement was not much different from our (^{3}He, t) resolution of $\approx$30 keV, which suggests that the comparison of this spectrum with our ^{44}Ca(^{3}He, t) spectrum should be straightforward.

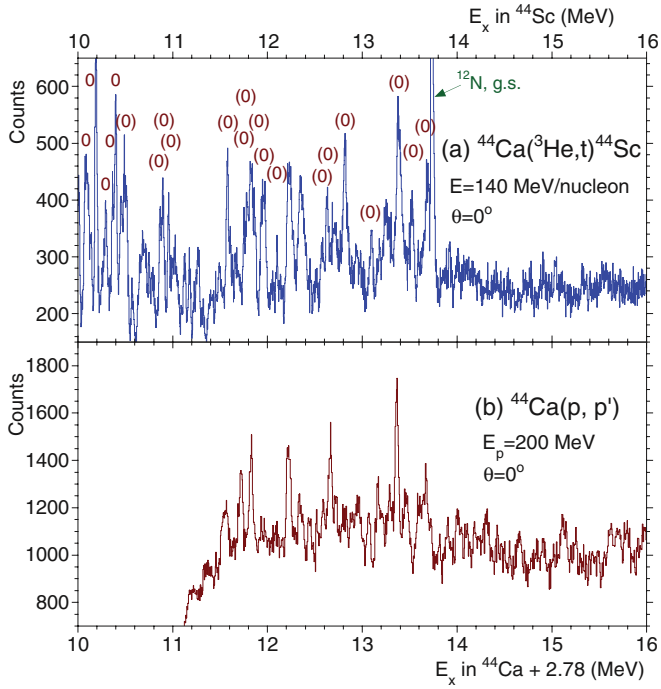

FIG. 7. (Color online) (a) The ^{44}Ca(^{3}He, t) spectrum of the E_x = 10–16 MeV region for events with scattering angles $\Theta \leqslant 0.5°$. States with or probably with $\Delta L = 0$ are indicated by "0" and "(0)," respectively. (b) The ^{44}Ca(p, p') spectrum measured at IUCF [59]. The measurements were carried out at E_p = 200 MeV and at very forward angles including 0° using the K600 spectrometer in transmission mode. The excitations in the $E_x > 8.3$ MeV region in ^{44}Ca were studied. We see several pairs of sharp peaks at the corresponding energies in the spectra. Note that the ordinates of both figures begin with finite counts to illustrate the structured part clearly.

In the ^{44}Ca(^{3}He, t), 0° spectrum showing the E_x = 10–16 MeV region [Fig. 7(a)], the states populated in $\Delta L = 0$ transitions and probably in $\Delta L = 0$ transitions are labeled "0" and "(0)," respectively. They are the candidates for GT states. The spectrum is compared with the ^{44}Ca(p, p') spectrum at 0° for the corresponding region shown in Fig. 7(b). As mentioned, spin-$M1$ states are prominent in the (p, p') measurement at 0°. The E_x scale of the ^{44}Ca(p, p') spectrum was determined by referring the E_x values of known spin-$M1$ states observed in the ^{28}Si(p, p') spectrum taken under the same conditions and shown in Ref. [59]. The E_x scale can have a systematic uncertainty of $\approx$30–50 keV.

The analog state of the g.s. of ^{44}Ca is the IAS in ^{44}Sc, and the IAS is observed at E_x = 2.779 MeV in the ^{44}Ca(^{3}He, t)^{44}Sc reaction. Therefore, the energy scale in Fig. 7(b) is shifted by 2.78 MeV to see the corresponding structure of the analogous spin-$M1$ and GT states.

Since the particle threshold opens only at 11.1 MeV [i.e., 13.9 MeV with the shifted energy scale of Fig. 7(b)] in ^{44}Ca, the continuum in the ^{44}Ca spectrum is instrumental (background). Therefore, in the ^{44}Ca(p, p') spectrum, depending on the method of background subtraction used in the analysis, the detection efficiency may not be equal all over the focal plane. However, several pairs of sharp peaks are apparently seen at the corresponding excitation energies in both spectra with uncertainties of 30–50 keV. We suggest that they are the analog states. In addition, we see that the prominent sharp peaks terminate at $\approx$ 13.7 MeV also in the (p, p') spectrum.

3. *Identification of isospin* T *of Gamow-Teller states*

Since the IAS of the g.s. of ^{44}Ca with $T = T_0 = 2$ is at E_x = 2.78 MeV in ^{44}Sc, we expect that the GT states with $T = 2$ are in the E_x = 9.8–13.8 MeV region in ^{44}Sc, while the $T = 3$, GT states are in the 14.3–17.3 MeV region, taking the excitation energies of the $T = T_0 = 2$ and the $T = T_0 + 1 = 3$, spin-$M1$ states discussed in Sec. IV C1 into consideration.

The expectation that the $T = 3$, GT states are situated higher than E_x = 14 MeV is supported by a recent observation of candidates for the $T = 3$, spin-$M1$ states in ^{56}Fe [60]. It is noted that the pf-shell nucleus ^{56}Fe has the same T_z value of +2 as ^{44}Ca and the g.s. has $T = T_0 = 2$. They compared the ^{56}Fe(^{3}He, t)^{56}Co and ^{56}Fe(p, p') spectra measured at 0°. By taking the differences of CG^2 values in exciting analog GT and spin-$M1$ states in these reactions into consideration [4,9,10], they could identify at least four candidates for the $T = 3$, spin-$M1$ states in the E_x = 11.5–13.7 MeV region of ^{56}Fe [61]. This finding suggests that the analog $T = 3$, GT states in the final $T_z = +1$ nuclei are situated higher by approximately these amounts of energy than the IAS. Adding the E_x value of 2.78 MeV of the IAS in ^{44}Sc, we can deduce that the $T = 3$, GT states in ^{44}Sc are in the region higher than 14.3 MeV.

As we see from Fig. 7, there are no sharp peaks above E_x = 13.7 MeV in ^{44}Sc, showing that the excitation of $T = 3$, GT states, if any, is very weak. Therefore, it is highly probable that the states observed with $\Delta L = 0$ character in ^{44}Sc in the region below E_x = 14 MeV are the GT states with either $T = 1$ or $T = 2$. In addition, if a corresponding state is also

observed in the ^{44}Ca(p, p') spectrum, the GT state should have $T = 2$. On the basis of the discussions outlined above, values of isospin T were examined for the GT states in the region above 11.5 MeV in ^{44}Sc, where the corresponding (p, p') data exist. The most probable T values are given in the last column of Table VI.

The observation that there is no obvious $T = 3$, GT strength suggests that the GT transition strength in the β^+ direction, that can be observed in (n, p)-type CE reactions, is also small. It should be noted that the GT transition strengths in the β^+ direction for pf-shell nuclei are of astrophysical interest in terms of deducing the electron-capture rate at the core-collapse stage of supernovae.

The weak $T = 3$, GT excitation can be understood in a simple SM picture of ^{44}Ca, i.e., the protons in the sd shell obey the $Z = 20$ shell closure and four extra neutrons are in the $f_{7/2}$ shell. In this picture, we find that there is no configuration that can make GT transitions in the β^+ direction. Accordingly, no (or only weak) excitations of the $T = T_0 + 1 = 3$, GT states are expected in the study of (n, p)-type CE reactions in the $T_z = +3$ nucleus ^{44}K (see Fig. 1). Accordingly, the excitations of the $T = 3$, analog GT states in ^{44}Sc in the ^{44}Ca$(^3$He$, t)$ reaction should also be weak assuming good isospin symmetry. In addition, the excitations of these $T = 3$ states in the (p, n)-type, $(^3$He$, t)$ reaction are further suppressed by the small value of CG^2 [4]. In the (p, n)-type reactions starting from the $T = T_0 = 2$ g.s., the CG^2 values are 3/5, 1/3, and 1/15, respectively, for the excitation of $T = 1$, 2, and 3 GT states. The CG^2 value, however, is unity for the excitation of the $T = 3$, GT states in (n, p)-type reactions.

The $M1$ states in ^{44}Ca was studied in an electron inelastic scattering experiment [62]. It is expected that the ^{44}Ca(e, e') experiment excites the same 1^+ states as observed in the ^{44}Ca(p, p') experiment, namely the analog states of the GT states in ^{44}Sc (see Fig. 1). However, they found no $M1$ states in the energy region $E_x = 8.2$–12.2 MeV, i.e., the region that corresponds to $E_x = 11.0$–15.0 MeV in ^{44}Sc. Their sensitivity limit for $M1$ transitions was $0.15\mu_N^2$ in $B(M1)$. This value corresponds approximately to $B(\mathrm{GT}) = 0.02$ in the ^{44}Ca$(^3$He$, t)^{44}$Sc reaction [4]. As we see from Table VI, almost all GT excitations observed in this region are weaker than the $B(\mathrm{GT})$ value of 0.02. Therefore, a higher sensitivity was needed in the ^{44}Ca(e, e') measurement to be able to see the corresponding $M1$ states.

D. Isospin mixing of the double isobaric analog state in ^{44}Ti

In the "$4n$ self-conjugate (even-even and $N = Z$, and thus $T_z = 0$)" nuclei, all particle decay channels of the lowest $T = 2$ state are isospin forbidden [20]. In ^{44}Ti, the first $T = 2$, 0^+ state, i.e., the double isobaric analog state (DIAS, see Fig. 1) of the g.s. of ^{44}Ca and ^{44}Cr, is located at $E_x = 9.338$ MeV, and it was found that the main γ-decay branch was to the $T = 1$, 1^+ state at 7.216 MeV [63]. These states are the analog states of the IAS at 2.779 MeV and the $T = 1$, 1^+ state at 0.667 MeV in ^{44}Sc, respectively. In addition, it was reported that the isospin forbidden α decay to the g.s. of ^{40}Ca has a branching ratio comparable with the isospin allowed γ decay [64], suggesting that the 9.338-MeV DIAS is isospin mixed.

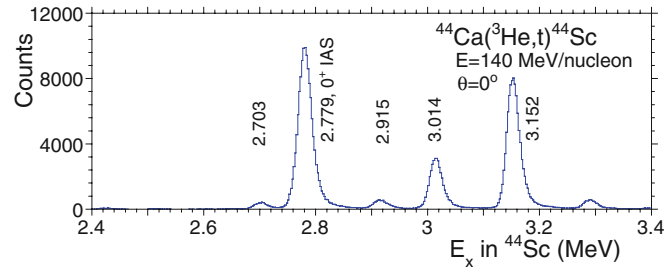

FIG. 8. (Color online) The 0°, ^{44}Ca$(^3$He$, t)^{44}$Sc spectrum showing the region around the IAS at 2.779 MeV.

It was found that a $J^\pi = 0^+$ subsidiary state is located at 9.298 MeV in ^{44}Ti, i.e., 40 keV below the DIAS, and its γ decay was studied in detail by Dixon *et al.* [65]. They suggested that these two states form an isospin-mixed doublet, and a mixing matrix element of 16(3) keV was derived. Although their γ-decay data and other experimental studies on these two states at 9.338 and 9.298 MeV are consistent with two-level mixing, it was not clear whether the subsidiary state at 9.298 MeV has the main isospin component of $T = 1$ or 0. Since the states in the $T_z = +1$ nucleus ^{44}Sc can be $T = 1$, but can never be $T = 0$, the existence or the nonexistence of the analog state of the 9.298-MeV subsidiary state in ^{44}Sc can answer this question, but the levels and γ transitions in ^{44}Sc [29] have not been studied in sufficient detail to reach a firm conclusion.

The IAS in ^{44}Sc, the single analog state of the $T = 2$, ^{44}Ca g.s., is located at 2.779 MeV. Therefore, we looked for a state with $\Delta L = 0$ character at around 2.739 MeV, i.e., 40 keV below the IAS, in the ^{44}Ca$(^3$He$, t)^{44}$Sc spectrum. As shown in Fig. 8, we could not find any candidate state in this region, where only $T = 1$ states can exist. Therefore, we suggest that $T = 0$ is the main component of the subsidiary state at 9.298 MeV in ^{44}Ti.

This is an interesting finding, because the report on the $\Delta T = 2$ isospin mixing is rather rare. In order to make such $\Delta T = 2$ mixing, two-step processes of isovector operators or an operator that is a second-rank tensor in isospin space is needed.

As is shown in the Appendix, by expanding the two-body Coulomb interaction, terms with isoscalar, isovector, and also the second-rank tensor in isospin space will appear [66]. Some exotic processes of nuclear interaction may also contribute. A quantitative estimation of the off-diagonal matrix element for the $\Delta T = 2$ mixing is a subject of interest.

In addition, from an experimental viewpoint, we should mention that in the present $(^3$He$, t)$ measurement a doublet with an energy difference of less than ≈ 7 keV is hard to recognize even with our resolution of 28 keV, especially if one of the states is only weakly excited. In order to come to a decisive conclusion, a more detailed structure study of ^{44}Sc, in particular the study of the γ decay of the 2.779-MeV IAS and its neighboring states, is needed.

In Ref. [67], $\Delta T = 2$ mixing has been reported in the study of particle decays of the $4n$ self-conjugate nucleus ^{40}Ca. Their measurement on the decay of the first 0^+, $T = 2$ state at 11.99 MeV in ^{40}Ca (i.e., the DIAS of the g.s. of ^{40}Ar and

^{40}Ti) showed that the α decay to the g.s. of ^{36}Ar is dominant over other branches such as proton decay or γ decay. The measured α-decay width was large and almost the same as the total decay width. Therefore, they came to the conclusion that the α-decay width arises from the mixing of the $T = 2$ DIAS with neighboring 0^+, $T = 0$ states. The appropriate sources of interactions or processes that cause the $\Delta T = 2$ mixing are, as mentioned, questions of interest.

V. SUMMARY

We carried out a ^{44}Ca(^{3}He, t)^{44}Sc experiment at the intermediate beam energy of 140 MeV/nucleon and scattering angles around 0°. The energy resolution of 28 keV ($\Delta E/E \approx 7 \times 10^{-5}$) allowed us to resolve many discrete states up to 13.7 MeV. It was found that the known $J^\pi = 1^+$, GT state at 0.667 MeV and also the $J^\pi = 0^+$ IAS at 2.779 MeV were prominent. These states showed forward-peaked angular distributions typical of $\Delta L = 0$ transitions. As a result of the angular distribution analysis for other excited states, it was found that the $\Delta L = 0$ strength, most probably GT strength, was highly fragmented.

Strongly excited states, particularly in the $\Theta \leqslant 0.5°$ spectrum, were found in the relatively low-lying region of $E_x < 6.2$ MeV and showed an angular distribution of $\Delta L = 0$. On the other hand, in the higher-energy region all of the states were weakly populated. In addition, above 14 MeV no structure involving discrete states was observed. Assuming that all of the states with $\Delta L = 0$ character, except the IAS, are GT states, the GT transition strengths B(GT) were derived using the proportionality between the GT cross section at 0° and the B(GT) value.

Under the assumption of isospin symmetry, we can deduce the properties of the exotic $T_z = -2 \rightarrow -1$, GT transitions from detailed studies of the $T_z = +2 \rightarrow +1$, GT transitions starting from stable nuclei. Note that the feeding ratios and thus the GT transition strengths are difficult to obtain in β-decay studies for short-lived $T_z = -2$ nuclei, but accurate half-lives $T_{1/2}$ have been measured even for these nuclei situated near the drip line. We first found that the β-decay half-life $T_{1/2}$ of ^{44}Cr can be reproduced from the distribution of the Fermi and GT transition strengths studied in the ^{44}Ca(^{3}He, t), CE reaction. In addition, the comparison of the ^{44}Ca(^{3}He, t)^{44}Sc spectrum and the ^{44}Cr $\rightarrow$ ^{44}V β-delayed proton spectrum suggested that these mirror GT transitions are in relatively good agreement in their energies as well as strengths, although one-to-one correspondence of the transitions could not be examined due to the limited energy resolution in the β-decay study. We suggest that the $T_z = +2 \rightarrow +1$, GT strength distribution obtained in the ^{44}Ca(^{3}He, t)^{44}Sc measurement provides a good estimate of the $T_z = -2 \rightarrow -1$, GT strength distribution. It should be noted that these GT transitions originating in proton-rich unstable nuclei are of astrophysical interest.

Starting from the $T = T_0 = 2$ g.s. of the $T_z = +2$ nucleus ^{44}Ca, the (^{3}He, t) reaction can populate GT states with $T = 1$, 2, and 3. On the other hand, the ^{44}Ca(p, p') reaction can excite spin-$M1$ states with $T = 2$ and 3, the analog states of the $T = 2$ and 3, GT states, respectively. By comparing the spectra from these reactions, several pairs of corresponding states were identified. Accordingly, we could assign $T = 2$ for the several weakly excited GT states in the $E_x = 11.5$–13.7 MeV region. No evidence was found for the $T = 3$ states.

It has been reported that the $T = 2$ DIAS of the g.s. of ^{44}Ca in ^{44}Ti forms an isospin-mixed doublet with a subsidiary state situated 40 keV below. We suggest that the subsidiary state has $T = 0$ judging from the non-existence of the corresponding state in the ^{44}Sc spectrum. Note that all states in the $T_z = +1$ nucleus ^{44}Sc have $T \geqslant 1$. This suggests mixing between the $T = 2$ and 0 states. To verify this interesting finding, a detailed study of the IAS region in ^{44}Sc, in particular by means of γ-ray spectroscopy, will be needed.

ACKNOWLEDGMENTS

The (^{3}He, t) experiments were performed at RCNP, Osaka University under the Experimental Program E307. The authors thank the accelerator group of RCNP for providing a high-quality ^{3}He beam. Y.F. acknowledges the discussions with Prof. W. Gelletly (Surrey), Prof. R.C. Johnson (Surrey), and Prof. P. von Brentano (Köln) for the preparation of this paper. Y.F. also acknowledges the support of MEXT, Japan under Grants No. 18540270 and No. 22540310. Y.F. and B.R. are grateful for the support of the Japan-Spain collaboration program by JSPS and CSIC. B.R., A.A., and E.E.A. are thankful for the support of Spanish Ministry under Grants No. FPA2005-03993, No. FPA2008-06419-C02-01, and No. FPA2011-24553. R.G.T.Z., J.D., C.J.G., R.M., and G.P. are grateful for the support of the U.S. NSF under Grants No. PHY-0606007 and No. PHY-0822648(JINA). E.G. acknowledges the support of the Istanbul University Scientific Research Projects Coordination Unit (BAP) under Projects No. NP 5626, No. UDP 7732, and No. UDP 26540, and E.G. and G.S. acknowledge the support of the Turkish Atomic Energy Authority (TAEK) under Project No. CERN-A5.H2.H1.01-4.

APPENDIX: EXPANSION OF THE TWO-BODY COULOMB INTERACTION

The Coulomb interaction between two nucleons is given by

$$V(1,2) = \frac{1}{2}[1 + \tau_3(1)]\,[1 + \tau_3(2)]\,\frac{e^2}{r_{12}}, \qquad \text{(A1)}$$

where $\tau_3 = -1$ for a proton and $+1$ for a neutron. As an operator in isospin space, we will show that this is a linear combination of a scalar, a vector, and a tensor of rank 2. It can, therefore, induce changes of isospin of 0, 1, and 2.

To see this we write

$$[1 + \tau_3(1)][1 + \tau_3(2)] = 1 + \tau_3(1) + \tau_3(2) + \tau_3(1)\tau_3(2). \qquad \text{(A2)}$$

The first term is an isoscalar and the second two terms are components of an isovector. The third term can be written as a combination of an isoscalar and a component of a second-rank tensor in isospin space using the identity

$$3\tau_3(1)\tau_3(2) = \vec{\tau}(1) \cdot \vec{\tau}(2) + \sqrt{6}\,[\vec{\tau}(1) \times \vec{\tau}(2)]_{2,0}. \qquad \text{(A3)}$$

The second term on the right, $[\vec{\tau}(1) \times \vec{\tau}(2)]_{2,0}$, is the $(2, 0)$ component of the second-rank tensor built out of the components of the isospin vectors $\vec{\tau}(1)$ and $\vec{\tau}(2)$, i.e.,

$$[\vec{\tau}(1) \times \vec{\tau}(2)]_{2,\mu} = \sum_{m,m'=0,\pm1} (1\, m\, 1\, m' \mid 2\, \mu)\tau_{1m}(1)\tau_{1m'}(2), \tag{A4}$$

where μ can be ±2, ±1, or 0. The Clebsch-Gordan coefficient in Eq. (A4) ensures that there are only contributions from m and m' values satisfying $\mu = m + m'$. The $\tau_{1m}(i)$, where $i = 1$ or 2, are isovector components defined by

$$\begin{aligned} \tau_{11} &= -\frac{1}{\sqrt{2}}(\tau_1 + i\tau_2), \\ \tau_{1-1} &= \frac{1}{\sqrt{2}}(\tau_1 - i\tau_2), \\ \tau_{10} &= \tau_3. \end{aligned} \tag{A5}$$

The operator $[\vec{\tau}(1) \times \vec{\tau}(2)]_{2,\mu}$ transforms like something with isospin 2. Therefore, the Coulomb interaction can mix states that differ in isospin by 0, 1, or 2.

[1] A. Bohr and B. R. Mottelson, *Nuclear Structure*, Vol. 1 (Benjamin, New York, 1969).

[2] F. Osterfeld, Rev. Mod. Phys. **64**, 491 (1992), and references therein.

[3] B. Rubio and W. Gelletly, in *The Euroschool Lectures on Physics with Exotic Beams Vol. III*, Lecture Notes in Physics Vol. 769 (Springer, Berlin, 2009), p. 99.

[4] Y. Fujita, B. Rubio, and W. Gelletly, Prog. Part. Nucl. Phys. **66**, 549 (2011), and references therein.

[5] K. Langanke and G. Martínez-Pinedo, Rev. Mod. Phys. **75**, 819 (2003).

[6] J. Rapaport and E. Sugarbaker, Annu. Rev. Nucl. Part. Sci. **44**, 109 (1994).

[7] T. N. Taddeucci, C. A. Goulding, T. A. Carey, R. C. Byrd, C. D. Goodman, C. Gaarde, J. Larsen, D. Horen, J. Rapaport, and E. Sugarbaker, Nucl. Phys. A **469**, 125 (1987), and references therein.

[8] W. G. Love, K. Nakayama, and M. A. Franey, Phys. Rev. Lett. **59**, 1401 (1987).

[9] T. Adachi, Y. Fujita, A. D. Bacher, G. P. A. Berg, T. Black, D. De Frenne, C. C. Foster, H. Fujita, K. Fujita, K. Hatanaka, M. Honma, E. Jacobs, J. Jänecke, K. Kanzaki, K. Katori, K. Nakanishi, A. Negret, T. Otsuka, L. Popescu, D. A. Roberts, Y. Sakemi, Y. Shimbara, Y. Shimizu, E. J. Stephenson, Y. Tameshige, A. Tamii, M. Uchida, H. Ueno, T. Yamanaka, M. Yosoi, and K. O. Zell, Phys. Rev. C **85**, 024308 (2012).

[10] H. Fujita, Y. Fujita, T. Adachi, A. D. Bacher, G. P. A. Berg, T. Black, E. Caurier, C. C. Foster, H. Fujimura, K. Hara, K. Harada, K. Hatanaka, J. Jänecke, J. Kamiya, Y. Kanzaki, K. Katori, T. Kawabata, K. Langanke, G. Martínez-Pinedo, T. Noro, D. A. Roberts, H. Sakaguchi, Y. Shimbara, T. Shinada, E. J. Stephenson, H. Ueno, T. Yamanaka, M. Yoshifuku, and M. Yosoi, Phys. Rev. C **75**, 034310 (2007).

[11] E. Ganioğlu, H. Fujita, Y. Fujita, T. Adachi, A. Algora, M. Csatlós, J. M. Deaven, E. Estevez-Aguado, C. J. Guess, J. Gulyás, K. Hatanaka, K. Hirota, M. Honma, D. Ishikawa, A. Krasznahorkay, H. Matsubara, R. Meharchand, F. Molina, H. Okamura, H. J. Ong, T. Otsuka, G. Perdikakis, B. Rubio, C. Scholl, Y. Shimbara, G. Susoy, T. Suzuki, A. Tamii, J. H. Thies, R. G. T. Zegers, and J. Zenihiro, Phys. Rev. C **87**, 014321 (2013).

[12] Y. Fujita, Y. Shimbara, I. Hamamoto, T. Adachi, G. P. A. Berg, H. Fujimura, H. Fujita, J. Görres, K. Hara, K. Hatanaka, J. Kamiya, T. Kawabata, Y. Kitamura, Y. Shimizu, M. Uchida, H. P. Yoshida, M. Yoshifuku, and M. Yosoi, Phys. Rev. C **66**, 044313 (2002).

[13] Y. Fujita, Y. Shimbara, A. F. Lisetskiy, T. Adachi, G. P. A. Berg, P. von Brentano, H. Fujimura, H. Fujita, K. Hatanaka, J. Kamiya, T. Kawabata, H. Nakada, K. Nakanishi, Y. Shimizu, M. Uchida, and M. Yosoi, Phys. Rev. C **67**, 064312 (2003).

[14] R. G. T. Zegers, H. Akimune, Sam M. Austin, D. Bazin, A. M. van den Berg, G. P. A. Berg, B. A. Brown, J. Brown, A. L. Cole, I. Daito, Y. Fujita, M. Fujiwara, S. Galès, M. N. Harakeh, H. Hashimoto, R. Hayami, G. W. Hitt, M. E. Howard, M. Itoh, J. Jänecke, T. Kawabata, K. Kawase, M. Kinoshita, T. Nakamura, K. Nakanishi, S. Nakayama, S. Okumura, W. A. Richter, D. A. Roberts, B. M. Sherrill, Y. Shimbara, M. Steiner, M. Uchida, H. Ueno, T. Yamagata, and M. Yosoi, Phys. Rev. C **74**, 024309 (2006).

[15] Y. Fujita, H. Akimune, I. Daito, H. Fujimura, M. Fujiwara, M. N. Harakeh, T. Inomata, J. Jänecke, K. Katori, A. Tamii, M. Tanaka, H. Ueno, and M. Yosoi, Phys. Rev. C **59**, 90 (1999).

[16] Y. Fujita, R. Neveling, H. Fujita, T. Adachi, N. T. Botha, K. Hatanaka, T. Kaneda, H. Matsubara, K. Nakanishi, Y. Sakemi, Y. Shimizu, F. D. Smit, A. Tamii, and M. Yosoi, Phys. Rev. C **75**, 057305 (2007).

[17] J. Rapaport, T. Taddeucci, T. P. Welch, C. Gaarde, J. Larsen, D. J. Horen, E. Sugarbaker, P. Koncz, C. C. Foster, C. D. Goodman, C. A. Goulding, and T. Masterson, Nucl. Phys. A **410**, 371 (1983).

[18] D. Wang, J. Rapaport, D. J. Horen, B. A. Brown, C. Gaarde, C. D. Goodman, E. Sugarbaker, and T. N. Taddeucci, Nucl. Phys. A **480**, 285 (1988).

[19] A. Bohr and B. Mottelson, *Nuclear Structure*, Vol. 2 (Benjamin, New York, 1975), Chap. 6, and references therein.

[20] *Isospin in Nuclear Physics*, edited by D. H. Wilkinson (North-Holland, Amsterdam, 1969).

[21] C. Dossat, N. Adimi, F. Aksouh, F. Becker, A. Bey, B. Blank, C. Borcea, R. Borcea, A. Boston, M. Caamano, G. Canchel, M. Chartier, D. Cortina, S. Czajkowski, G. de France, F. de Oliveira Santos, A. Fleury, G. Georgiev, J. Giovinazzo, S. Grévy, R. Grzywacz, M. Hellström, M. Honma, Z. Janas, D. Karamanis, J. Kurcewicz, M. Lewitowicz, M. J. López Jiménez, C. Mazzocchi, I. Matea, V. Maslov, P. Mayet, C. Moore, M. Pfützner, M. S. Pravikoff, M. Stanoiu, I. Stefan, and J. C. Thomas, Nucl. Phys. A **792**, 18 (2007).

[22] See web site http://www.rcnp.osaka-u.ac.jp

[23] T. Wakasa, K. Hatanaka, Y. Fujita, G. P. A. Berg, H. Fujimura, H. Fujita, M. Itoh, J. Kamiya, T. Kawabata, K. Nagayama, T. Noro, H. Sakaguchi, Y. Shimbara, H. Takeda, K. Tamura, H. Ueno, M. Uchida, M. Uraki, and M. Yosoi, Nucl. Instrum. Methods Phys. Res. A **482**, 79 (2002).

[24] M. Fujiwara, H. Akimune, I. Daito, H. Fujimura, Y. Fujita, K. Hatanaka, H. Ikegami, I. Katayama, K. Nagayama, N. Matsuoka, S. Morinobu, T. Noro, M. Yoshimura, H. Sakaguchi, Y. Sakemi, A. Tamii, and M. Yosoi, Nucl. Instrum. Methods Phys. Res. A **422**, 484 (1999).
[25] T. Noro *et al.*, RCNP (Osaka University) Annual Report, 1991 (unpublished), p. 177.
[26] Y. Fujita, K. Hatanaka, G. P. A. Berg, K. Hosono, N. Matsuoka, S. Morinobu, T. Noro, M. Sato, K. Tamura, and H. Ueno, Nucl. Instrum. Methods **126**, 274 (1997), and references therein.
[27] H. Fujita, G. P. A. Berg, Y. Fujita, K. Hatanaka, T. Noro, E. J. Stephenson, C. C. Foster, H. Sakaguchi, M. Itoh, T. Taki, K. Tamura, and H. Ueno, Nucl. Instrum. Methods Phys. Res. A **469**, 55 (2001).
[28] H. Fujita, Y. Fujita, G. P. A. Berg, A. D. Bacher, C. C. Foster, K. Hara, K. Hatanaka, T. Kawabata, T. Noro, H. Sakaguchi, Y. Shimbara, T. Shinada, E. J. Stephenson, H. Ueno, and M. Yosoi, Nucl. Instrum. Methods Phys. Res. A **484**, 17 (2002).
[29] J. Chen, B. Singh, and J. A. Cameron, Nucl. Data Sheets **112**, 2357 (2011).
[30] Y. Ichikawa, T. K. Onishi, D. Suzuki, H. Iwasaki, T. Kubo, V. Naik, A. Chakrabarti, N. Aoi, B. A. Brown, N. Fukuda, S. Kubono, T. Motobayashi, T. Nakabayashi, T. Nakamura, T. Nakao, T. Okumura, H. J. Ong, H. Suzuki, M. K. Suzuki, T. Teranishi, K. N. Yamada, H. Yamaguchi, and H. Sakurai, Phys. Rev. C **80**, 044302 (2009).
[31] DW81, a DWBA computer code by J. R. Comfort (1981) used in an updated version (1986), an extended version of DWBA70 by R. Schaeffer and J. Raynal (1970).
[32] S. Y. van der Werf, S. Brandenburg, P. Grasdijk, W. A. Sterrenburg, M. N. Harakeh, M. B. Greenfield, B. A. Brown, and M. Fujiwara, Nucl. Phys. A **496**, 305 (1989).
[33] R. Schaeffer, Nucl. Phys. A **164**, 145 (1971).
[34] R. G. T. Zegers, H. Abend, H. Akimune, A. M. van den Berg, H. Fujimura, H. Fujita, Y. Fujita, M. Fujiwara, S. Galés, K. Hara, M. N. Harakeh, T. Ishikawa, T. Kawabata, K. Kawase, T. Mibe, K. Nakanishi, S. Nakayama, H. Toyokawa, M. Uchida, T. Yamagata, K. Yamasaki, and M. Yosoi, Phys. Rev. Lett. **90**, 202501 (2003); S. Y. van der Werf and R. G. T. Zegers (private communication).
[35] T. Yamagata, H. Utsunomiya, M. Tanaka, S. Nakayama, N. Koori, A. Tamii, Y. Fujita, K. Katori, M. Inoue, M. Fujiwara, and H. Ogata, Nucl. Phys. A **589**, 425 (1995).
[36] T. Adachi, Y. Fujita, P. von Brentano, G. P. A. Berg, C. Fransen, D. De Frenne, H. Fujita, K. Fujita, K. Hatanaka, M. Honma, E. Jacobs, J. Kamiya, K. Kawase, T. Mizusaki, K. Nakanishi, A. Negret, T. Otsuka, N. Pietralla, L. Popescu, Y. Sakemi, Y. Shimbara, Y. Shimizu, Y. Tameshige, A. Tamii, M. Uchida, T. Wakasa, M. Yosoi, and K. O. Zell, Nucl. Phys. A **788**, 70c (2007).
[37] Y. Fujita, J. Phys. Conf. Ser. **20**, 107 (2005).
[38] T. Adachi, Y. Fujita, P. von Brentano, A. F. Lisetskiy, G. P. A. Berg, C. Fransen, D. De Frenne, H. Fujita, K. Fujita, K. Hatanaka, M. Honma, E. Jacobs, J. Kamiya, K. Kawase, T. Mizusaki, K. Nakanishi, A. Negret, T. Otsuka, N. Pietralla, L. Popescu, Y. Sakemi, Y. Shimbara, Y. Shimizu, Y. Tameshige, A. Tamii, M. Uchida, T. Wakasa, M. Yosoi, and K. O. Zell, Phys. Rev. C **73**, 024311 (2006).
[39] L. Popescu, T. Adachi, G. P. A. Berg, P. von Brentano, D. Frekers, D. De Frenne, K. Fujita, Y. Fujita, E.-W. Grewe, M. N. Harakeh, K. Hatanaka, E. Jacobs, K. Nakanishi, A. Negret, Y. Sakemi, Y. Shimbara, Y. Shimizu, Y. Tameshige, A. Tamii, M. Uchida, H. J. Wörtche, and M. Yosoi, Phys. Rev. C **79**, 064312 (2009).
[40] Y. Fujita *et al.*, RCNP (Osaka University) Annual Report, 2010 (unpublished), p. 1.
[41] Y. Fujita *et al.*, RCNP (Osaka University) Annual Report, 2010 (unpublished), p. 2.
[42] T. N. Taddeucci, J. Rapaport, C. C. Foster, C. D. Goodman, C. Gaarde, J. Larsen, C. A. Goulding, D. J. Horen, T. Masterson, and E. Sugarbaker, Phys. Rev. C **28**, 2511 (1983).
[43] M. Honma, T. Otsuka, B. A. Brown, and T. Mizusaki, Phys. Rev. C **69**, 034335 (2004).
[44] M. Honma, T. Otsuka, T. Mizusaki, M. Hjorth-Jensen, and B. A. Brown, J. Phys.: Conf. Ser. **20**, 7 (2005).
[45] J. Jänecke, K. Pham, D. A. Roberts, D. Stewart, M. N. Harakeh, G. P. A. Berg, C. C. Foster, J. E. Lisantti, R. Sawafta, E. J. Stephenson, A. M. van den Berg, S. Y. van der Werf, S. E. Muraviev, and M. H. Urin, Phys. Rev. C **48**, 2828 (1993).
[46] Y. Shimbara, Y. Fujita, T. Adachi, G. P. A. Berg, H. Fujimura, H. Fujita, K. Fujita, K. Hara, K. Y. Hara, K. Hatanaka, J. Kamiya, K. Katori, T. Kawabata, K. Nakanishi, G. Martìnez-Pinedo, N. Sakamoto, Y. Sakemi, Y. Shimizu, Y. Tameshige, M. Uchida, M. Yoshifuku, and M. Yosoi, Phys. Rev. C **86**, 024312 (2012).
[47] K. Ikeda, S. Fujii, and J. I. Fujita, Phys. Lett. **3**, 271 (1963).
[48] M. Ichimura, H. Sakai, and T. Wakasa, Prog. Part. Nucl. Phys. **56**, 446 (2006), and references therein.
[49] F. Pougheon, J. C. Jacmart, E. Quiniou, R. Anne, D. Bazin, V. Borrel, J. Galin, D. Guerreau, D. Guillemaud-Mueller, A. C. Mueller, E. Roeckl, M. G. Saint-Laurent, and C. Détraz, Z. Phys. A **327**, 17 (1987).
[50] Y. Fujita, T. Adachi, P. von Brentano, G. P. A. Berg, C. Fransen, D. De Frenne, H. Fujita, K. Fujita, K. Hatanaka, E. Jacobs, K. Nakanishi, A. Negret, N. Pietralla, L. Popescu, B. Rubio, Y. Sakemi, Y. Shimbara, Y. Shimizu, Y. Tameshige, A. Tamii, M. Yosoi, and K. O. Zell, Phys. Rev. Lett. **95**, 212501 (2005).
[51] J. C. Hardy and I. S. Towner, Phys. Rev. C **71**, 055501 (2005).
[52] D. H. Wilkinson and B. E. F. Macefield, Nucl. Phys. A **232**, 58 (1974).
[53] W. G. Love and M. A. Franey, Phys. Rev. C **24**, 1073 (1981).
[54] E. Lipparini and S. Stringari, Phys. Rep. **175**, 103 (1989).
[55] R. Leonardi, Phys. Rev. C **14**, 385 (1976).
[56] C. Djalali, N. Marty, M. Morlet, A. Willis, J. C. Jourdain, N. Anantaraman, G. M. Crawley, A. Galonsky, and P. Kitching, Nucl. Phys. A **388**, 1 (1982).
[57] C. Djalali, N. Marty, M. Morlet, A. Willis, J. C. Jourdain, N. Anantaraman, G. M. Crawley, A. Galonsky, and J. Duffy, Nucl. Phys. A **410**, 399 (1983); **417**, 84 (1984).
[58] A. Willis, M. Morlet, N. Marty, C. Djalali, D. Bohle, H. Diesener, A. Richter, and H. Stein, Nucl. Phys. A **499**, 367 (1989).
[59] D. J. Mercer, G. M. Crawley, S. Danczyk, A. Galonsky, J. Wang, A. Bacher, G. P. A. Berg, A. C. Betker, W. Schmidt, and E. J. Stephenson, IUCF Science and Technology Report 1994–1995, Indiana University (unpublished), p. 20, https://scholarworks.iu.edu/dspace/handle/2022/459/browse?value=Mercer%2C+D. J.&type=author
[60] M. Nagashima, Y. Shimbara, H. Fujita, Y. Fujita, T. Adachi, N. T. Botha, E. Ganioğlu, K. Hatanaka, K. Hirota, N. T. Khai, H. Matsubara, K. Nakanishi, R. Neveling, H. Okamura, H. J. Ong, Y. Sakemi, Y. Shimizu, G. Susoy, T. Suzuki, A. Tamii,

J. Thies, and M. Yosoi, in *The 10th International Symposium on Origin of Matter and Evolution of Galaxies, Osaka, March 2010*, edited by I. Tanihara *et al.*, AIP Conf. Proc. No. 1269 (AIP, New York, 2010), p. 427.

[61] Y. Shimbara (private communication).

[62] W. Steffen, H.-D. Gräf, W. Gross, D. Meuer, A. Richter, E. Spamer, O. Titze, and W. Knüpfer, Phys. Lett. B **80**, 23 (1980).

[63] J. J. Simpson, W. R. Dixon, and R. S. Storey, Phys. Rev. Lett. **29**, 1472 (1972).

[64] S. J. Freedman, C. A. Gagliardi, M. A. Oothoudt, A. V. Nero, R. G. H. Robertson, F. J. Zutavern, E. G. Adelberger, and A. B. McDonald, Phys. Rev. C **17**, 2071 (1978).

[65] W. R. Dixon, R. S. Storey, and J. J. Simpson, Phys. Rev. C **18**, 2731 (1978).

[66] R. C. Johnson (private communication).

[67] S. K. B. Hesmondhalgh, E. F. Garman, D. M. Pringle, S. H. Chew, W. N. Catford, and K. W. Allen, Phys. Lett. B **183**, 35 (1987).